FINAL REPORT

Submitted to
U.S. Department of Justice
Danielle McLeod-Henning, Program Manager
General Forensics R&D Program
Office of Investigative and Forensic Sciences
National Institute of Justice

GRANT NO: 2012-DN-BX-K046

TSI GO# 4T088

Brass Board Forensic Crime Scene Survey Camera

Submitted by
Technical PI: Milind Mahajan
805-373-4888 (phone); 805-373-4105 (fax)
Email: milind.mahajan@teledyne.com

Contributors: Milind Mahajan, Karen Zachery, Weiya Zhang, Steven Chen, John Mansell
Andrew Brackley, Erik Andrews

Submission Date: January 31st, 2015

DUNS 96-795-3613
EIN 52-231-4487

Recipient Organization
Teledyne Scientific & Imaging, LLC
1049 Camino Dos Rios
Thousand Oaks, CA 91360

Grant Period: January 1st, 2013 - December 31st 2014
Technical work began on July 17th 2013

Reporting Period End Date: December 31st 2014
Report Term or Frequency: Final

Abstract

Contrast enhancement techniques that use forensic light sources (FLS) with spectral bandpass filters, off-axis illumination (for finger prints, shoe prints), and fluorescence imaging (for bio-fluids), are powerful tools already in use by the forensic community. However the majority of current instruments and procedures are labor intensive, require a darkened environment, and pose significant logistical challenges for field application. Our concept of a stand-off multi-spectral camera combined with a compact strobed and gated illuminator can provide:

1) Multiple detection capabilities in a single camera system
2) Ability to operate in presence of ambient light in multi-spectral and fluorescence modes
3) Ability to enhance detection using advanced image-processing algorithms
4) Intuitive, nearly real time presentation of the analysis, overlaid on the scene imagery

The result will be increased speed of crime scene investigation, and reduced contamination of crime scene. It will assist planning and prioritization of further investigation, and significantly reduce labor-intensive non real-time image processing. We note that our system even when fully developed is not intended to be and cannot be a substitute for detailed laboratory work. It is intended to act as a "triage tool" that will work similar to a point-and-shoot camera, thus serving to detect and prioritize evidence for more detailed analysis.

The goal of currently funded work is to develop and test an improved, compact, brass board crime-scene-imaging camera that builds upon a previous successful proof-of-concept breadboard level demonstration (NIJ grant 2010-DN-BX-K144) through specific hardware improvements, and provision for a graphical user interface (GUI). The goal for the brass board hardware is to reach a maturity level enabling operation and testing by a subject matter expert after additional training and support from Teledyne Scientific and Imaging (TSI) personnel.

The specific hardware upgrades accomplished under the current project are:

1) A TSI developed agile (continuously tunable) electro-optic spectral bandpass filter with nominally 10X higher transmission over the current state of the art at the ultraviolet (UV)/Blue end of the spectrum. The filter is also capable of high transition speed (nominally 10X faster than the current state of the art) achieved using a novel, dual-frequency drive electronics.
2) Nominally 6X brighter illuminator using COTS LED and collimation options
3) Three additional illumination wavelengths (9 total)
4) Portable semi-custom drive electronics
5) 6X higher resolution camera (12 MP)
6) Graphical user interface for image acquisition to enable collection of user-defined imaging recipes
7) Graphical user interface for post processing and analysis of the image sequences

The emphasis was to maximize (within the constraints of the project) performance, portability; and provide a versatile, easy to use, GUI that allows image processing and visualization of the results of contrast enhancement algorithms.

The hardware is now fully functional. The GUIs for image acquisition and analysis are fully functional. We have proven the functionality through imaging and algorithmic enhancement

examples. The hardware and software development consumed more resources than we anticipated; which prevented us from imaging a more extensive set of simulated targets.

This report describes in detail, the hardware and GUI design, fabrication, and functionality provided to the user. We illustrate functionality through examples. We conclude with thoughts on the path forward, which includes market analysis for an integrated crime scene survey camera and for a high-transmission, high-speed tunable filter that can be used as an accessory for cameras, light source or microscopy.

Table of Contents

Executive Summary

The forensic community employs numerous contrast enhancement techniques that use forensic light sources (FLS) with multiple wavelength filters, off-axis illumination for prints, and fluorescence imaging for bio-fluids. However, all of these techniques require a darkened environment, which is often a significant logistical challenge. Furthermore, there are scenarios where logistics (e.g. a closed highway) or available resources (e.g. crimes of less serious nature) can restrict the amount of time spent by an expert at the crime scene. Post processing and visualization is a laborious and time consuming process.

There is need for a camera that enables a practitioner to effectively visualize, prioritize, and guide data collection and processing beyond what current tools can do. There is a need for a tool that can rapidly survey a crime scene and provide nearly real time (~1 second processing time, not video rate) information to help plan and prioritize the investigation. A recent DoJ grant [1] enabled us to establish the feasibility of a broadly capable, affordable, multispectral forensic imaging tool. We used an optical breadboard based entirely on off-the-shelf components to analyze targets of interest to forensic investigators such as inks, chemical solvent stains, blood, saliva, latent prints etc. The imaging modalities included multispectral, fluorescence and polarization imaging. We tested an array of contrast enhancement algorithms against collected imagery that exploit multi-spectral color, texture, and polarization signatures of the targets, and used adaptive dynamic range compression and false coloring to optimally render the (processed or unprocessed) images. TSI's contrast enhancement algorithms are inspired by biological principles of signal interaction in the retinal circuits. Our multispectral processing is analogous to the techniques used for remote sensing surveys. Encouraged by the positive results, we proposed and undertook development of a significantly enhanced brass board multi-spectral camera.

The specific hardware developments realized under the current grant were guided by the breadboard experimentation results. We added illumination channels in both UV, visible and near infrared (NIR) wavelengths. We increased the illumination intensity by a factor of six for better range and improved background suppression. This substantial increase in both number of wavelengths and brightness was accomplished through integration of off-the-shelf LEDs, collimation optics, and custom drive electronics as opposed to the packaged "LED spotlights" that we used for the breadboard.

We had noted that UV and blue wavelengths were particularly effective for imaging biological fluids, and had identified the need for a liquid crystal tunable filter (LCTF) to replace the filter wheel. The LCTF is a continuously tunable band pass filter where the control voltages on the device establish the center wavelength for imaging. Liquid crystal technology development has been driven by the display industry and is restricted primarily to visible wavelengths. Off-the-shelf LCTF solutions have extremely low transmission at long-wave UV and blue wavelengths (~2% at 375 nm- with relevant bandwidth) and insufficient free spectral range (< 1 octave) to cover UV and NIR wavelengths simultaneously. They also exhibit slow switching speed for NIR capable filters.

TSI leveraged its considerable knowhow in optimizing liquid crystal device structures to overcome all of the above limitations and was able to construct an LCTF with >20% transmission at 375 nm (>10X improvement over the current state of the art), a free spectral range that covers long wave UV to NIR operation (375 nm to 850 nm), and a dual frequency drive capability that achieves switching speeds of 12 ms (~10X improvement over the current

state of the art). **We consider our demonstration of this high performance tunable filter to be an enabling development for the forensic survey camera.**

We upgraded from the 2 Megapixel (2 MP) camera (on the breadboard) to a 12 MP GigE monochrome camera and continued to use the Genoptic/ CoastalOpt UV-Vis-NIR lens.

We developed two separate graphical user interfaces: one for image acquisition and the other for algorithmic image enhancement, analysis and viewing.

The image acquisition GUI allows the user to create and edit a recipe (a sequence of images). A sequence contains a user specified number of images with user specified illumination wavelengths and LCTF state for each of those images. If the user wants to capture traditional multispectral data, the illuminator and LCTF are at the same wavelengths. If the user wants to capture traditional fluorescence data, the illumination wavelength is kept constant and the LCTF scans wavelengths greater than illumination wavelength. Upon completion of the image sequence capture, the GUI stores the sequence in a directory dedicated to the sequence. Image names include the illuminator state, LCTF state, and exposure time. An image preview is available to the user during the data collection.

The image analysis GUI allows the user to load the sequences and manipulate the imagery via analysis panels that use the algorithms demonstrated in the previous project. The GUI currently relies on a fair number of user inputs. We would like to increase the level of automation in the future by using the quality metric analysis [see page 32] to select images with the highest information content and perform contrast enhancements through use of a knowledge base that selects algorithms most likely to produce the best results based on the target. The basic building blocks for increased future automation are in place. Table 1 summarizes the benefits of the upgrades.

Table 1. Accomplished hardware & software enhancements

Component	**Breadboard**	**Brassboard (current)**	**Performance enhancement benefit**
Camera	2MP	12 MP	Higher resolution images
Filter	Mechanical wheel	Tunable electro-optic	Fast, compact, very large number receive channels
Illuminator	6 COTS spotlights 6 wavelengths	55 LED modules and 9 wavelengths	Enhanced spectral differentiation, 6X brightness improvement
Drive electronics	COTS	Semi-custom	Compact and portable
User interface	None	GUI	Enable an outside person to operate/test with some training

Dissemination of results, market analysis (for both an integrated forensic survey camera and a standalone LCTF) and technology transition planning are expected to follow in the upcoming months.

(a)

(b)

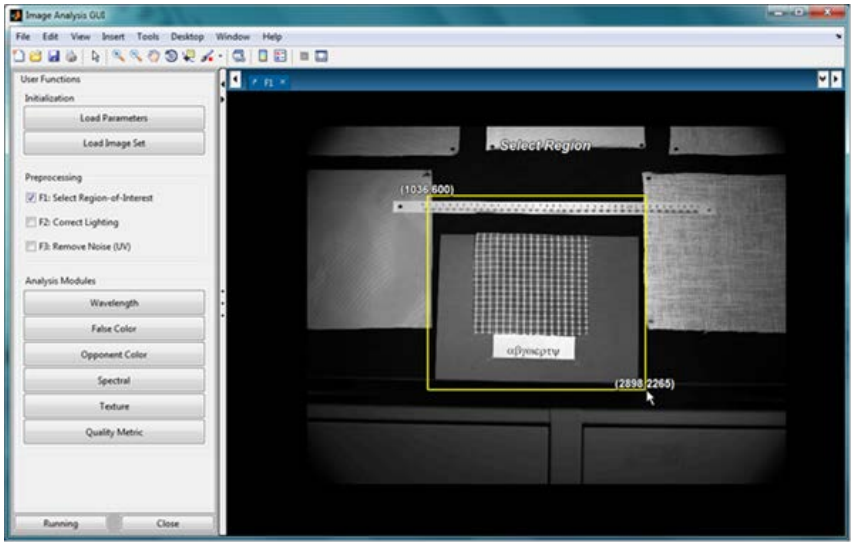

(c)

Figure 1. Brassboard forensic crime scene survey camera system

(a) Camera with LCTF mounted on the lens, (b) VIS-NIR (left) and UV (right) illuminators, (c) Image processing GUI

Main Body of the Final Technical Report

I. Introduction

I.1. Background

Crime scene investigators are tasked with detecting several types of materials present at the scene, including body fluids, hair, fiber, gunshot residue, explosive residue, imprints, and glass and metal shards. These are often difficult to distinguish from the background and present a formidable challenge in detection and identification. Some examples are blood on rust, shoeprints on glossy surfaces, stains on similarly colored backgrounds and textures that create overwhelming clutter.

A review of the literature on established techniques and forensic products reveals some major operational deficiencies. Digital single lens reflex (DSLR) cameras (e.g. Nikon D700, or Kodak 760) along with powerful image processing tools (e.g. Adobe Photoshop) have proven extremely valuable in the field [2]. However, a significant amount of manual post-processing work is required for image enhancement. Conventional DSLRs do not capture image signatures outside the visible spectrum. Recently, specialized monochrome forensic SLR cameras have become available for detection of ultra-violet (UV) and near infrared (NIR) wavelengths [3]. These are used in conjunction with various optical filters. NIR capability has been shown to be useful in enhancing the visibility of blood stains, document-forgery, and gunpowder residue [3,4].

Another tool popular among forensic investigators is the use of a forensic light source (FLS). FLS may be based on an arc lamp [5], LED [6], or even laser [7] typically used with a matching set of filters, or simply colored eyewear [5]. Imaging with FLS is particularly sensitive to background illumination and requires a darkened environment. UV reflectance has been shown to be useful for fingerprint, bite mark, bruise, and shoeprint identification [8]. A large class of materials (e.g. body fluids) exhibits fluorescence, which is also exploited [9, 10].

Extreme oblique angle illumination with FLS is often used to examine light scattered by shoeprints, fingerprints etc. [11] Polarization signatures have also been shown to be useful in certain scenarios [12]. Recently a new class of scene documentation instruments, capable of 3D imaging of crime scene using a scanning LIDAR [13] or a scanning camera [14] has also become available.

Different materials comprising crime scene evidence of interest have different signatures, and thus require a plethora of techniques for contrast enhancement; there is no single, integrated device that combines even a few of these techniques. There is a lack of sensors with an ability to detect and enhance evidence, within a wide crime scene area in a short period of time at stand-off distances to minimize the potential for contamination of the scene. Finally, manual data collection with multiple sensors and laborious post processing in the lab are time intensive operations and restrict rapid location, identification, and quantitative analysis of crime scene data in real time.

Sunlight poses overwhelming interference for nearly all FLS imaging techniques and the resultant requirement of darkening the area imposes logistical constraints. There is a critical need for nearly real time analysis that is not sensitive to ambient illumination. Nearly real time analysis will enable agile re-planning and collection of additional crime scene data based on the analysis.

Work performed by TSI on the earlier grant [1] points toward a crime scene survey camera approach that addresses some key shortcomings of current approaches. TSI demonstrated a proof of concept breadboard imaging system containing commercial off-the-shelf (COTS) components. We tested the system with a variety of simulated crime scene evidence samples (we will refer to these as "imaging targets") and applied TSI-developed image processing algorithms. We demonstrated significant contrast enhancement and improved detection thresholds across the board. We achieved the goal of establishing a proof of concept and performed an initial trade study involving an evaluation of diverse samples. We restricted the breadboard to strictly COTS components and chose affordability over performance. These choices also restricted the trade study to an indoor environment.

Our assessment of the trade study and feedback from subject matter experts encouraged us to continue further development towards a field portable imaging device.

I.2. Research Rationale

Recent advances and improved availability of high brightness LEDs spanning the entire UV through NIR wavelength spectrum, availability of sensitive monochrome cameras and TSI's resident expertise of producing a high transmission, wide free spectral range, tunable bandpass filter, has enabled development of a single portable imaging system with multiple detection capabilities. Background rejection through spectral filtering and temporal gating enables operation in the presence of ambient light. Modern image processing and rendering algorithms allow the user to view multiple image modalities and exploit the results immediately in the field by making informed decisions on next steps.

The focus of the current effort is to improve the maturity level from an all COTS, optical bench, proof of concept experimentation to a semi-custom, portable, well packaged imaging system hardware with a sufficiently user friendly software package that will enable demonstration and testing outside TSI Laboratory (possibly by subject matter experts with some training).

The intent of this research is not to match the performance of existing laboratory systems and techniques in every respect but to develop an easy to use, field portable imager that possesses a substantial fraction of capabilities, normally only available in the laboratories.

II. Methods

II.1.Hardware Description

The three subsystems that constitute the brass board forensic camera hardware are: 1) Camera with a multispectral lens, 2) Illuminators with associated drive electronics, and 3) A tunable electro-optic filter (LCTF) with associated drive electronics.

Figure 2 shows the functional diagram of the hardware.

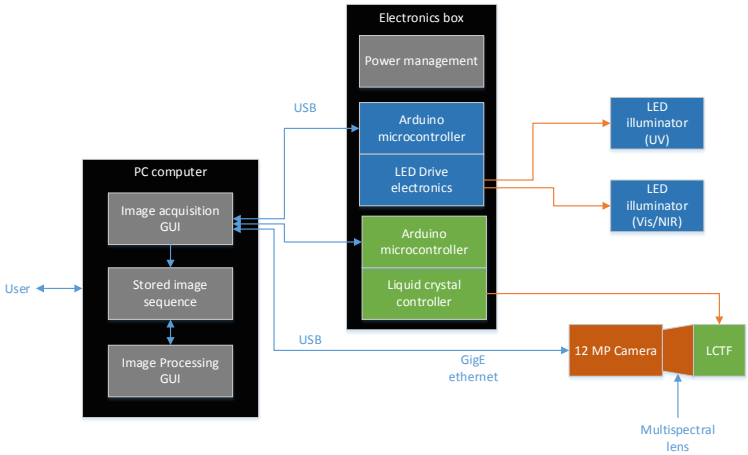

Figure 2. Functional diagram of the brassboard system

II.1.1. Camera and Multispectral Lens

True monochrome SLRs, while highly desirable, are no longer easily available. We were left with two choices for the camera 1) An SLR with IR-UV cut filters removed by a third party vendor (RGB filters cannot be removed) or 2) a scientific or instrumentation grade monochrome camera (no RGB filters). We used a large format 12 MP (4096×3072) monochrome machine vision camera from Teledyne DALSA which allows full format frame rate of 2 fps with 10 bit depth. Our prior experience indicated that 10 bits are generally sufficient for algorithmic enhancements, and for critical high dynamic range (HDR) scene, we can support an exposure bracketed HDR image. While a higher (14 bit) dynamic range large format monochrome camera is a possible hardware upgrade, the cost was not affordable for this project.

Conventional lenses do not transmit well outside the visible band. They also need focus adjustment. Manual focus will disturb image capture and automatic focus between shots is time consuming. We continued using the CoastalOpt® UV-VIS-IR 60 mm lens from Jenoptic. This high performance lens eliminated the need to change the focus during imaging. The camera and lens combination provides a 21.1°×15.8° field of view (FOV), sufficient to capture a large section of the scene, without compromising resolution.

II.1.1. LED Based Illumination

In line with the proposal, we designed the illumination with a larger number of wavelength options (nine wavelengths spaced fairly evenly through long wave UV to NIR) and a significantly higher intensity output (nominally 6X).

The proof of concept breadboard experiment used packaged LED spotlights and their associated programmable COTS drive electronics. While convenient for a bench top experiment, this approach did not scale up well in terms of size, weight and cost. We chose to design a semi-custom illuminator using discrete components, namely: power LED dies mounted on metal-core printed circuit boards, plastic collimators that are compatible with the power LED modules, high current drivers, multi-channel relays and an Arduino microcontroller (an open-source hardware board designed around an 8-bit Atmel AVR microcontroller) .

We narrowed down the high power LED emitter suppliers from about one dozen to two. We purchased and evaluated 14 different LED models (at multiple wavelengths), 3 different types of optics, and a compact high power LED driver. The selection criteria include luminous flux, comprehensiveness of the wavelengths offered, availability of matching COTS optics, and ease of integration. Furthermore, we considered the phenomenology related to certain wavelengths reported in literature [15-26].

Table 2 summarizes nine down-selected wavelengths, manufacturer and number of modules for each required to reach the desired illumination level. Table 3 shows the matching optical lenses for the selected LEDs. As we are limited to COTS lenses for collimation, the field angle of these lenses are the closest we could find to the field of view of the camera. The full width at half maximum (FWHM) of UV LEDs was less than desired. For the purpose of this project we have the option of restricting the camera FOV, or locating the illuminator farther to compensate for this limitation imposed by COTS availability. We split the illuminator into two: One for UV and one for VIS-NIR wavelengths to allow users to locate them at two different distances from the target, if so desired.

Table 2. Down-Selected LED Emitter Modules

Wavelength (nm)	Manufacturer	Number of diodes in a module	Number of Modules	Power density at 1m (w/o over driving) W/m^2
365	LED Engin	1	11	21.8
400	LED Engin	1	3	30
470	Philips Lumileds	3	4	25.8
530	Philips Lumileds	3	8	22.4
590	Philips Lumileds	3	9	35.8
627	Philips Lumileds	3	4	22.4
655	Philips Lumileds	3	3	20.8
740	LED Engin	4	8	21
850	LED Engin	4	6	15

Table 3. Available Optics for LED Emitters

Wavelengths	Supplier	FWHM (of cone angle)	Material	Size (mm)
UV	Ledil	12°	COP (High UV transmission)	21.6 dia×15.1 ht
Vis	Carlo	27°*	Polycarbonate	20 dia×6 ht
NIR	LED Engin	37°*	PMMA	38.9 dia×19.2 ht

* Exceed full FOV of camera

We measured the emission spectra of the selected LED emitters using a spectrometer. The result is shown below in Figure 3.

The spectral bandwidth of 591 nm LED is larger than anticipated but it is nearly completely overlapped by the selected LCTF pass band and we do not believe the spectral width differences to be a concern.

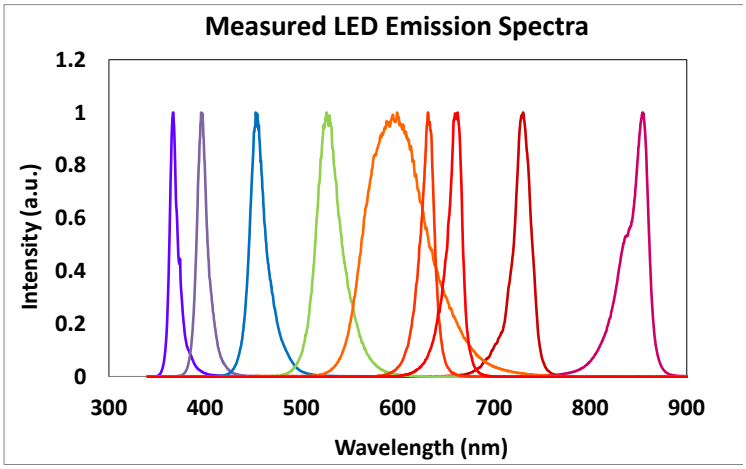

Figure 3. Emission spectra of the selected LEDs

We assembled the LED emitters with their matching lenses using a temporary fixture, and used a custom made goniometer to measure their luminous intensity distribution. The measured luminous intensity distribution is shown in Figure 4. 200 mA DC of drive current was used throughout these measurements. Minor variation of the FWHM angles is evident in both figures. This is the result of the chromatic effects in lens materials.

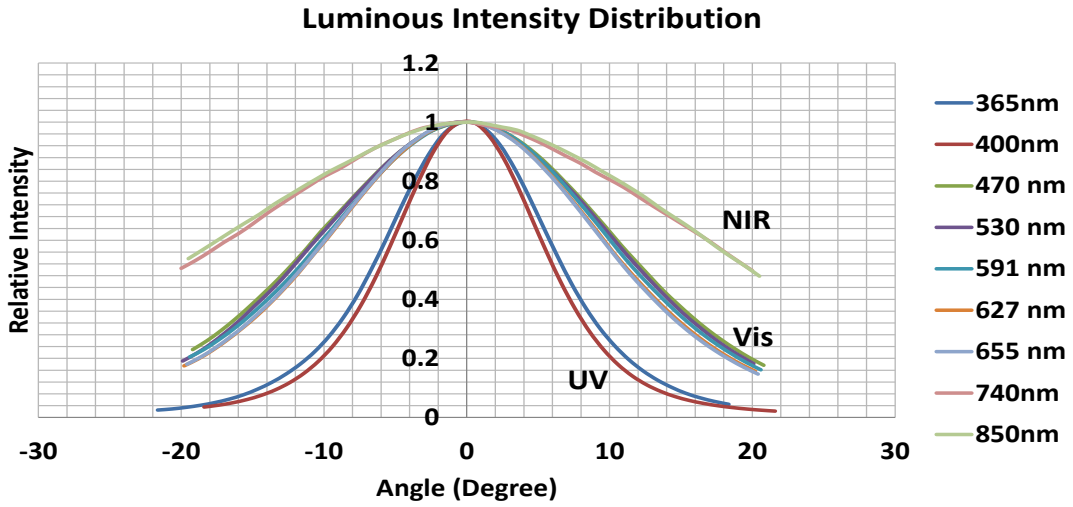

Figure 4. Luminous intensity distributions of LED/Lens combination

Vis/NIR cone angle exceeds camera FOV. UV does not; implying for UV wavelengths, camera may operate in a windowed mode, or UV illuminator will be located farther for the purpose of this project.

We also measured on-axis light power densities of the LED/ lens pairs at 1 m distance from the front of the modules with 700 mA DC driving currents. Results are summarized in Table 4. For easy comparison, radiometric units are used for all wavelengths. The purpose of these measurements is to select the number of LEDs of each color for the illuminator, and compare the output with the LEDs used on the breadboard camera project [1]. We note the substantially higher on axis power at individual LED levels across the board.

Table 4. Measured on-axis light power densities of the single LED /lens pairs at 1 m and comparison to the prior project (2010-DN-BX-K144)

LED Supplier	Wavelength (nm)	Power density (W/m^{-2})
Current project (brassboard)		
LED Engin	365	1.98
	400	10.00
	740	2.62
	850	4.54
Philips Lumileds	470	6.45
	530	2.80
	591	3.98
	627	5.61
	655	6.92
Previous project (breadboard)		
StockerYale (breadboard LED)	374	0.7375
	467	0.596875
	517	0.6875
	629	2.3875
	736	1.1125
	860	1.26875

Multiple choices are available for COTS drivers. We chose and tested the Luxdrive A009-D-V-2100 BuckBlock high output wide range LED power module by LED dynamics. It offers up to 2100 mA constant drive current to the LEDs in a small form factor (2.0”x1.2”x0.38”), as well as pulse and strobe capabilities that are easy to integrate.

We tested the functionality of the BuckBlock LED driver on an electrical breadboard. The number of LEDs which can be driven in parallel is limited by the maximum output current of the driver, which is 2100mA. For the selected LEDs, two or three branches can be driven simultaneously in parallel, depending on the desired driving current (700 mA typical but can be overdriven to 1000 mA). The number of LEDs

that can be driven in series is limited by the maximum DC output voltage of the driver, which is equal to the input voltage and has an absolute maximum rating of 32 V. The typical forward voltages of the selected LEDs range from 2 to 5 V per diode. Since each LED emitter may consist of three (Philips Lumileds) or four (LED Engin) diodes, two or three emitters can be driven in series in general.

We used a combination of Buckblock LED drivers (constant current sources) and a 16 channel relay module to design drive electronics. We used an Arduino microcontroller (an open-source hardware board designed around an 8-bit Atmel AVR microcontroller) to control timing of the analog drivers and switches based on user input. This controller is able to accept serial commands from the PC computer where the image acquisition and processing GUIs reside. The schematic of illuminator drive electronics is shown in Figure 5.

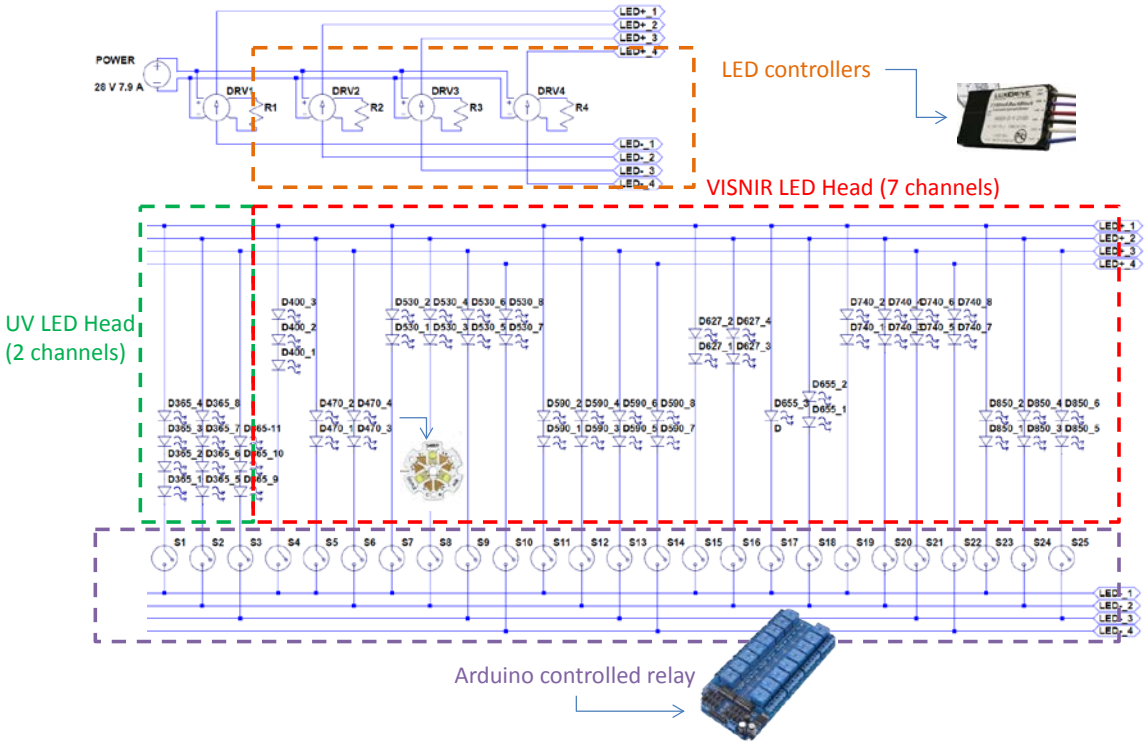

Figure 5. Schematic for components making up the two LED illuminator drive electronics

Arduino single board microcontroller is used to turn a specific wavelength channel on or off as desired. The controller accepts serial commands from laptop computer where the image acquisition and processing GUIs reside.

We programmed the microcontroller that when powered up, awaits commands from the USB serial port. It supports a number of simple commands such as switch ON wavelength channel X, Switch off wavelength channel X, Probe current state, Strobe a channel for fixed time duration, etc. These commands are called by the image acquisition GUI as needed for the data collection.

The electronics resides in an enclosure with long leads running to the illuminator heads. The UV head consists of 14 LED modules, while the Vis-NIR head consists of 42 LED modules. The next problem we tackled was creating a distribution of these LEDs on the illuminator heads that

produces a circularly symmetric and reasonably uniform illumination pattern at a few meters distance.

We developed illuminator layouts using Zemax raytrace software and a Visual Basic interface that allowed us to vary the layout and analyze the resultant illumination pattern. The resultant final configuration is shown in Figure 6.

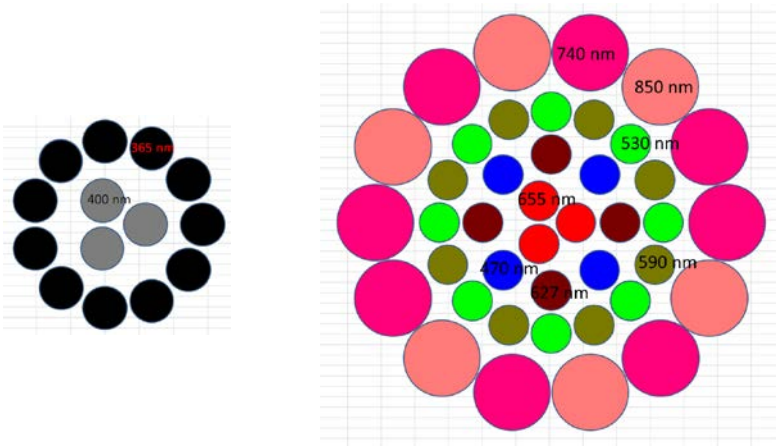

Figure 6. Arrangement of LEDs of different wavelengths in two illuminator modules UV (left) VIS-NIR (right)

For simplicity, each emitter was modeled as a disc emitter with diameter equal to the collimation optic diameter. The disc emits in a hemisphere with a distribution of the rays symmetric about the local z axis, as defined by a cubic spline fit to intensity vs. angle data. The aggregate intensity at nominal illumination distances was found and verified to have no structure beyond a circularly symmetric spot, slowly weakening in intensity as a function of distance away from the center. This slow monotonic behavior will enable normalization of illumination in the image processing software. See Figure 7.

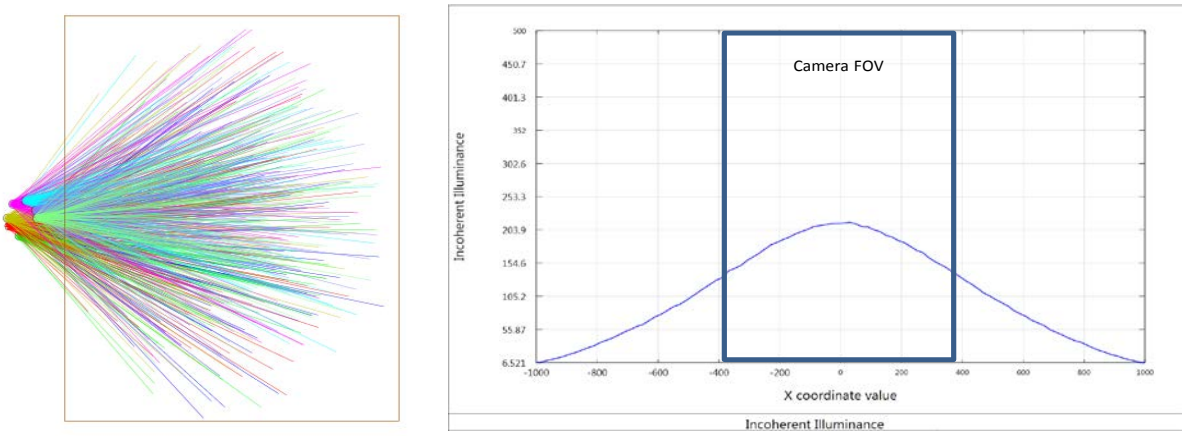

Figure 7. Zemax raytrace analysis of illuminator configuration for 740 nm wavelength.

Left shows illustration of ray trace. Right shows cross-section of intensity at 1.5 meters distance. It is a well behaved distribution that will be normalized over the camera field of view (FOV) during image processing

II.1.1. Liquid Crystal Tunable Filter

The liquid crystal tunable filter (LCTF) is an electro-optic (no moving parts) tunable bandpass filter that replaces the mechanical 6-position filter wheel from the breadboard. This device was custom built at TSI along with the associated drive electronics. It is packaged so it can be threaded to the front of the imaging lens. It is substantially more compact and has continuous tunability within its free spectral range to select the receive wavelength band. It

works with polarized light, which means half the light from the illuminator is not used unless the illuminator is polarized. On the other hand polarization imaging is possible via rotation of the filter with respect to camera body. While constructing polarized illumination or polarization recovery in light sources is certainly feasible [27], it is beyond the scope of this project. We rely entirely on high intensity of illumination and high polarized transmission of the filter to meet the image SNR needs. While LCTF components are available off the shelf [28, 29], their short wavelength transmission is well below that required for the proposed application.

LCTF: The primary performance challenges for a liquid crystal tunable filter are:

1. High transmission at short wavelengths (UV/blue – current off-the-shelf state of the art ~2% at 375 nm). Short wavelengths are important for forensic targets particularly when the system is used in fluorescent mode.
2. Large free spectral range (off-the-shelf state of the art 400-700 nm). For brassboard camera we operate from long wave UV (365 nm) to near IR (850 nm).
3. Fast response time (off-the-shelf state of the art for NIR cells ~150 ms)

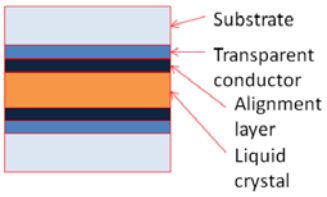

Figure 8. Cross section of a liquid crystal cell

Not to scale, TSI demonstrated high transmission and fast speed through materials optimization and dual frequency drive electronics

Figure 8 shows a typical liquid crystal cell, a basic building block of an LCTF. It has a thin (several microns) layer of liquid crystal sandwiched between two glass substrates. The glass substrates are coated with a transparent conductor (typically Indium Tin Oxide- ITO) and an alignment layer, both sub-microns thick. Liquid crystal technology development has been driven by the display industry, which is concerned with visible wavelengths and the materials used in the industry have severe absorptive and/or reflective losses at short wavelengths (UV and short wavelength blue). Multi-cell architectures make the loss management even more critical. Response of a liquid crystal cell is dependent on its material elastic constant and is inversely proportional to square of thickness of the liquid crystal layer. An LCTF requires cells that are significantly thicker than found in displays, and longer wavelengths need higher thickness, which really limits the response times. TSI has expertise in optimizing liquid crystal cells outside of visible range (e.g. short wave IR (SWIR) [30, 31]. TSI also leveraged an unconventional dual frequency addressing scheme used for SWIR wavelength devices to demonstrate LCTF speed improvement.

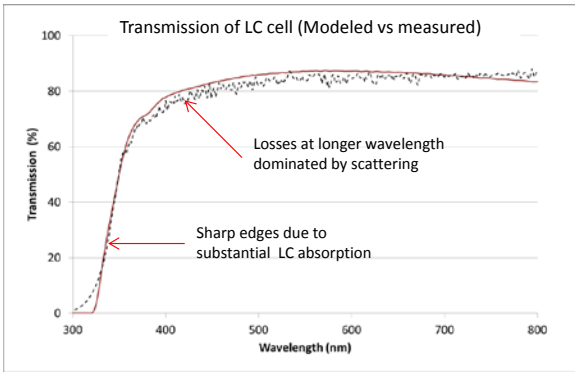

Figure 9. Transmission of LC cell

The model (dotted line) is in good agreement with measurement (solid line). This picture includes Fresnel loss.

An LCTF is essentially a multi-layer birefringent filter where the birefringence of each layer can be tuned to correspond to a desired wavelength. Other birefringent filter design approaches include Lyot filters, Solc filters, etalons etc. [32, 33] Conventional

birefringent filters use alternating stack of layers of liquid crystal cells and polarizers. Lyot and Solc designs use a large number of liquid crystal cells but only two polarizers.

We down-selected the most promising LC cell materials through spectrophotometric measurements over UV-Vis-NIR wavelengths. We quantified component level losses related to materials and mechanisms (absorption, reflection, and scattering) at short wavelengths, and developed a loss model. Our detailed model using TFCalc thin film design software is able to accurately predict the transmission loss of a cell at different wavelengths [Figure 9]. We found that liquid crystal cells have lower transmission than UV optimized polarizers and thus selected a conventional birefringent filter approach over the Lyot/Solc approach.

We modelled the birefringent filter using GNU Octave (provides functionality similar to Matlab under GNU general public license). During the design we realized that the strong dispersion of the birefringence (particularly at the short wavelengths due to absorption in the UV) severely restricts the free spectral range of the filter. See Figure 10.

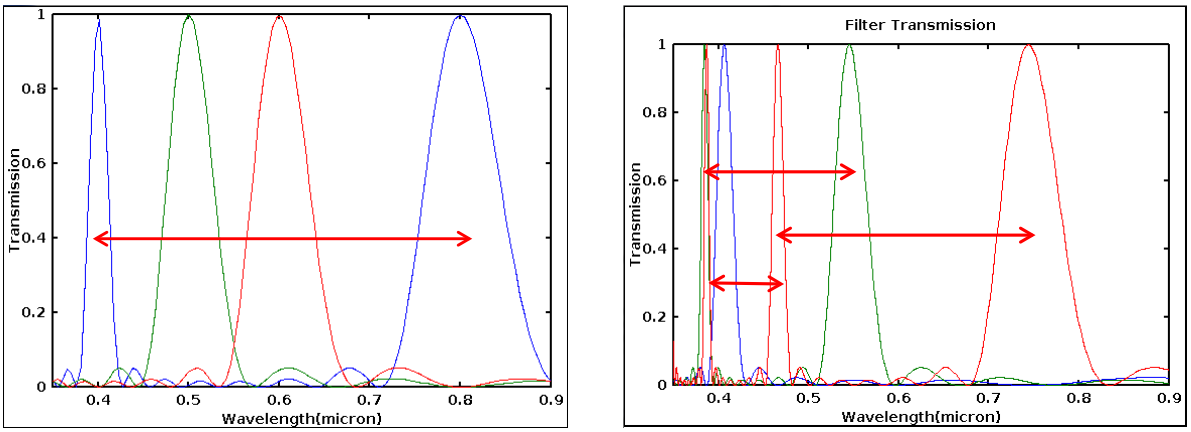

Figure 10. FSR and dispersion of birefringence

(Left) One octave of FSR with zero dispersion (Right) Severely limited birefringence due to dispersion of refractive index/ birefringence

Our design uses 5 stages, arranged to produce a bandpass response that envelops the LED emission spectra, as well as suppress side lobes that will otherwise limit the free spectral range (useful bandwidth). In the process we sacrificed some transmission in the NIR, but this is not a concern as the material transmission in the NIR is significantly higher than in the UV/Blue regions. See Figure 11.

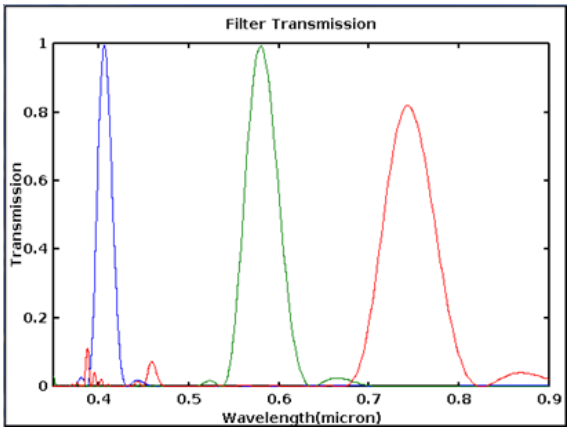

Figure 11. Filter design with large FSR
Some transmission in NIR is traded for larger FSR

We fabricated and characterized individual LC cells for their birefringence vs voltage response with a HeNe laser (633 nm). We explored characterizing the birefringence at individual LED wavelengths but this creates a complication due to the large spectral bandwidth of the LED emission, and makes it difficult to decipher the birefringence voltage

relation reliably.

We assembled an alternating stack of cells and polarizers to build the multi-stage filter. We placed the filter between the source and detector of a fiber coupled spectrophotometer from Ocean Optics and applied appropriate voltages derived from HeNe measurements to form a bandpass filter at 633 nm. We then tuned the voltages manually to shift the bands to lower wavelengths. Figure 12 shows the measured transmission data and a comparison with an off-the-shelf filter. While we were limited in the spectrophotometer operational range, the data clearly shows the absorption edge pushed far lower in UV to achieve significantly higher transmission.

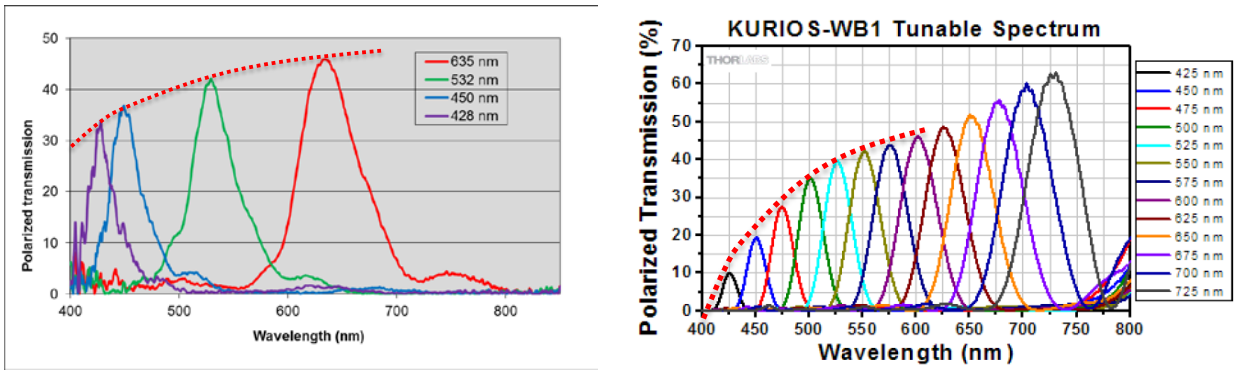

Figure 12. Comparison of TSI filter measurement (left) with off-the-shelf LCTF from Thorlabs (right)

TSI filter is optimized for short wavelengths. While we were limited in the spectrophotometer operational range, the data very clearly shows the absorption edge pushed far lower in UV to achieve significantly higher transmission. Transmission in NIR is somewhat lower.

The transmission achieved at the shorter wavelengths is impressive. Another off the shelf filter produced by Perkin Elmer [29] also appears comparable to the Thorlabs filter in terms of transmission. After accounting for an estimated number of stages in the off-the-shelf filters, we estimate our filter to be > 10X transmission at 375 nm. **This is an enabling development not just for the forensic crime scene camera (due to an extensive phenomenology present at the shorter wavelengths) but as a potential standalone product.**

We fabricated an electronic board that is capable of driving up to 10 liquid crystal cells using ether single frequency (slow) or dual frequency (fast) addressing modes with output voltages up to nominally 36 V ac. The slowest transition in the filter is limited by ability of the thickest liquid crystal cell to switch from one edge of the FSR to other (nominally 1 octave). Our measurements on the slowest (thickest) liquid crystal stage indicate an ability to switch within 12

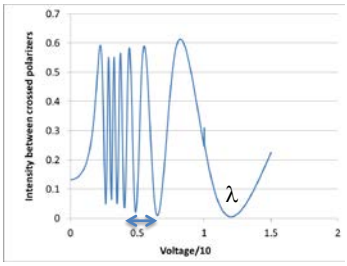

Switching thru two octaves
=2λ @ 633 nm

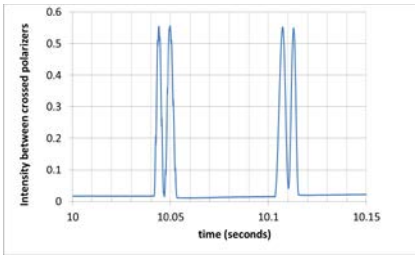

Dual frequency kicking achieves ~12 ms speed
Speed without "kicking" was 300 ms for this transition

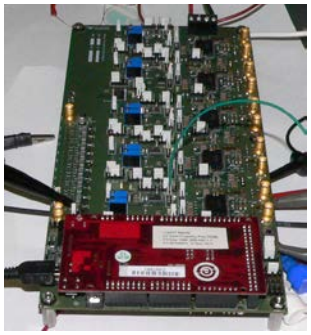

Figure 13. Dual frequency drive can achieve high speed transition of filter state

Custom 10-channel driver card is shown in the photograph on the right.

ms by incorporating 20 volt pulses to accelerate the transitions, with potential to switch even faster with higher drive voltage. See Figure 13. Off-the-shelf devices operating in NIR wavelengths have switching times of nominally 150 ms [29].

At the heart of the filter driver is another Arduino microcontroller that is connected via USB serial interface to the computer where the image acquisition GUI resides. The image acquisition GUI has access to the file that stores the acquisition sequence and the filter calibration data, which defines the number of filter states and corresponding control voltages. Currently we have nine defined Rx filter states that line up with the nine transmit wavelengths. In principle, there is no restriction to the number of Rx states as the filter is continuously tunable. The image acquisition GUI loads the relevant data into the controller and orchestrates an imaging sequence over the serial connection.

II.2.Hardware Integration and Packaging

We tested and verified functionality of camera, illuminators and LCTF modules and associated controllers independently of each other. We packaged the electronics in a compact portable enclosure (~13.5”wide×6”tall×13.5”deep). This electronics enclosure requires one AC and one DC power input. Connectors are provided for serial connection to two Arduino controllers (to the computer where image acquisition GUI resides) and three analog cables (to two illuminators and one LC filter). We built and tested the wiring harness (3 multi-conductor cables and two off-the-shelf USB cables). The electronics enclosure also has an integrated temperature controller that can be used to monitor the LCTF temperature and maintain it within the operating window. Figure 14 and Figure 15 show the front and the back of the electronics enclosure.

Figure 14. Controller electronics enclosure (back panel)

Rear panel of the enclosure shows connections for USB cables to PC computer, multi-conductor cables to illuminators and LC filter (LCTF), power inputs etc.

Figure 15. Integrated semi-custom electronics (inside and the front panel)

Inside of the enclosure includes microcontroller boards, relays, LC driver board, bipolar power supply, LED drivers, and temperature controller.

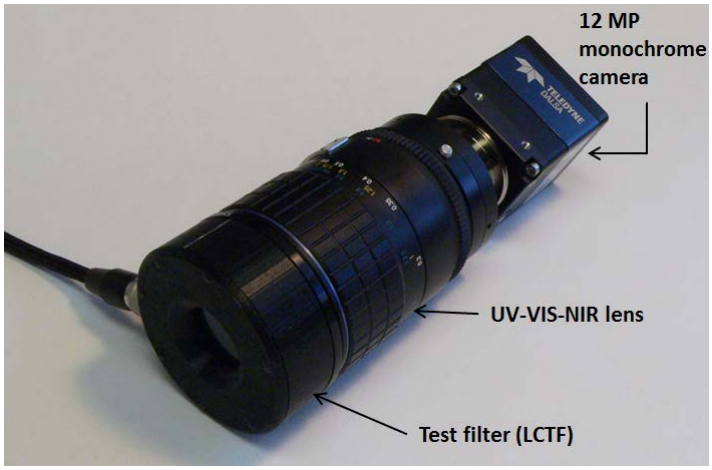

Figure 16. LCTF mounted to the UV-VIS-NIR lens and 12 MP camera

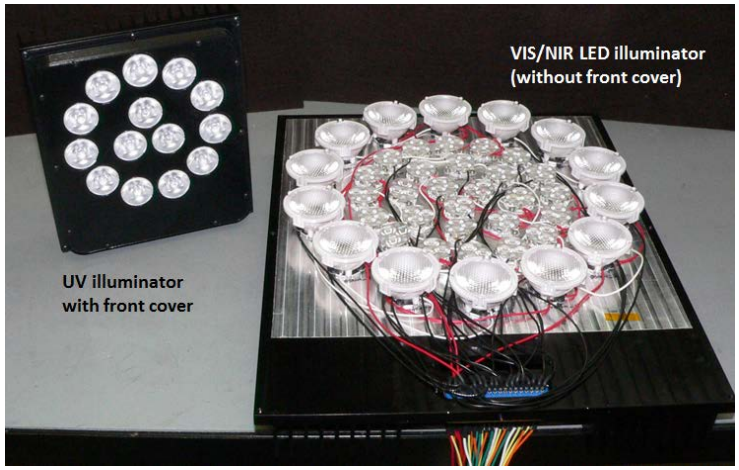

Figure 17. Multispectral LED illuminators

We packaged the LCTF in a mount that screws onto the front threads of the UV-Vis-NIR imaging lens. See Figure 16.

We glued the illuminator LED modules and collimation optics onto aluminum panels that also serve as heat sinks. A front cover was added for aesthetic reasons. Quarter-twenty threaded holes are provided for convenient mounting to standard photography tripods. See Figure 17.

II.3.Software

II.3.1. Image Acquisition GUI

Our image collection is written in C# and runs on a Windows PC. It allows users to create and edit a recipe (a sequence of images). A sequence can contain any number of images where the user specifies the number of images and the illumination and received wavelength (LCTF state) for each of the images. If the user wants to capture traditional multispectral data, then the illumination and LCTF wavelengths are to be the same. If the user wants to capture traditional fluorescence data, the illumination wavelength is kept constant and the LCTF scans all wavelengths greater than the illumination wavelength.

When the capture image button is pressed, the GUI sequentially goes through the recipe. It switches ON the illuminator, takes a few frames to determine the correct exposure time, collects the image, and saves it as a 16 bit raw file with exposure time, illumination and filter (LCTF) wavelengths appended in the file name. Each sequence is stored in a separate directory where the image processing GUI can access it. An image preview is available to the user as the data collection is taking place. See Figure 18.

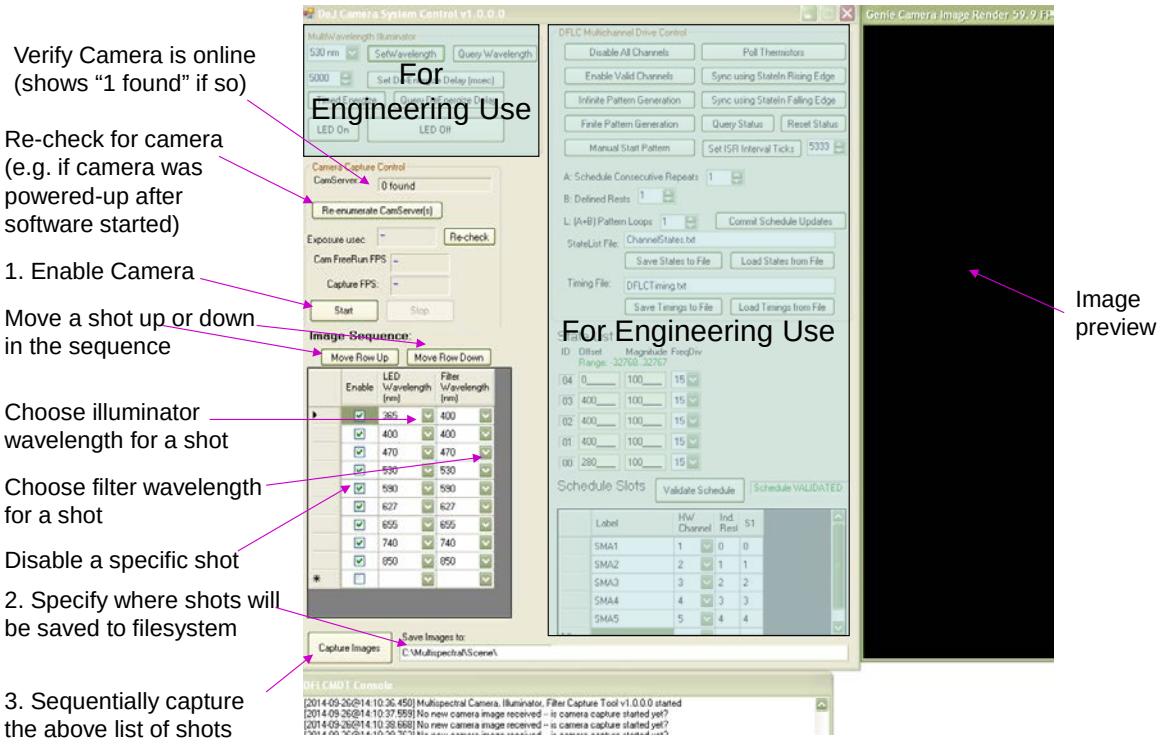

Figure 18. Image Acquisition GUI

II.3.2. Image Analysis GUI

GUI Specifications and Design

Our data analysis software (GUI, I/O, algorithms) runs under the Windows 7 operating system on a 64-bit, Intel-based laptop computer. The software operates as a stand-alone module separate from the camera hardware and software components. The GUI infrastructure was developed in the MATLAB® programing environment using Java Swing libraries as well as extensions from the SwingLabs SwingX Project. Java Swing libraries provide a less restrictive set of widgets and tools for creating a much richer GUI than those generally provided with MATLAB® built-in unicontrol tools. By using MATLAB® as the underlying programing language as opposed to C# or C++, m-file functions and scripts developed under the previous project [1] could be directly integrated into the GUI framework without the need for compiling dynamic link libraries. This decision helped streamline the process of code integration and software modifications.

Our data analysis software provides a user friendly environment that allows a user to easily access imagery collected with the crime scene survey camera, and execute different analysis components. The GUI architecture permits users to interactively select an image, define a sequence of data analysis algorithms, and enter algorithm input parameters through the use of programmable constructors, such as panels, pull-down menus, edit/check boxes, and push-buttons. The GUI automatically loads an image into the MATLAB® workspace, executes selected algorithm sequences, displays results to the computer monitor, and outputs image-based results in a standard image format for documentation purposes. Output results are displayed and organized using tab constructors to provide a quick and easy mechanism for viewing results. All data analysis modules were designed around the standard panel layout shown in Figure 18. This strategy was incorporated into our design process to help unify operating procedures for the selection and execution of analysis algorithms.

The algorithms incorporated within the Data Analysis GUI rely on the following MathWorks MATLAB® toolboxes: Image Processing Toolbox, Signal Processing Toolbox, Statistics Toolbox, and Optimization Toolbox. In addition, several algorithms also utilize shareware toolboxes.

Standard Panel Layout

The standard panel layout used for all data analysis modules is shown in Figure 19. The figure window is divided into two main components: input panel and output panel. The two regions are separated by a divider bar which can be interactively repositioned to increase the width of either panel. The two small arrows at the top of the divider let the user collapse (and then expand) either of the panels with a single click. The divider can also be repositioned by simply dragging it with the mouse left to right. Note that, when the divider is dragged, the screen continually updates.

The user input panel is further subdivided into two regions: user parameter and module functions. These regions are populated with pull-down menus, edit/check boxes, and push-buttons, which allow the user to configure and execute the various data analysis algorithms. Results (images) generated by the various algorithms are displayed in the output panel.

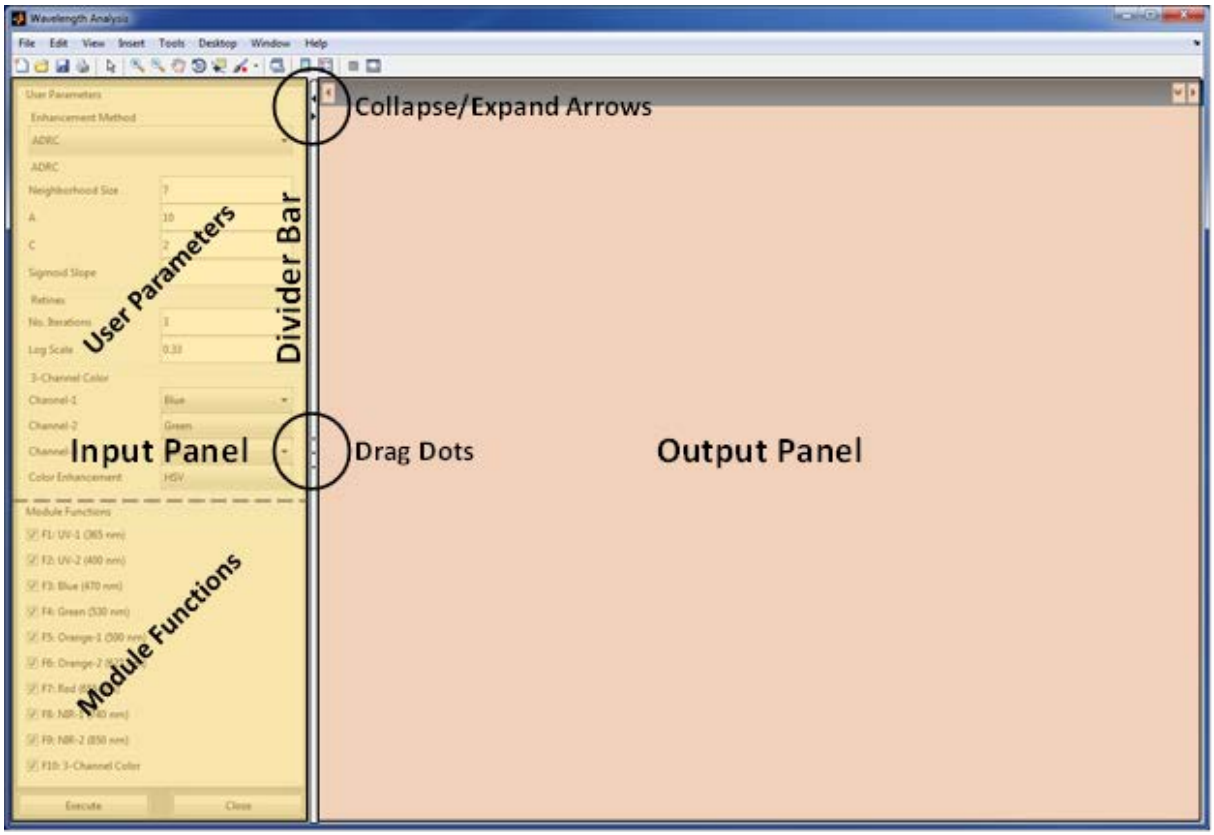

Figure 19. Standard layout for data analysis panels

The figure window is divided into two main panels: input (left) and output (right). Panel widths can be changed using either the collapse/expand arrows or drag dots located on the divider bar. The input panel is subdivided into the user parameter (top) and module functions (bottom) regions. This is where interactive constructs such as pull-down menus, edit/check boxes, and push-buttons are located to allow for user inputs. The output panel is the region where algorithm results (images) are displayed.

User Parameters

The *User Parameters* region of a data analysis panel is where the user changes/sets algorithm parameters. User inputs in this region are provided by means of pull-down menus and text edit boxes similar to those shown in Figure 20. Text edit boxes are designed to prevent the user from entering invalid values. Some parameters, such as band combinations used in multispectral processing, are dependent on specific illuminator wavelengths being present in a given data set. For these parameters, the range of valid values is actively determined by the current data set. An example of this is illustrated in Figure 20 with *3-Channel Color*. Here we see that only seven of the nine illuminator wavelengths present in the crime scene survey camera are listed in the *Channel-1* pull-down menu. Orange-2 and Red are missing from the list of wavelengths to reflect the fact that the current data set is void of these channels. This strategy was incorporated into our GUI design to help guide the user in his/her selection of values.

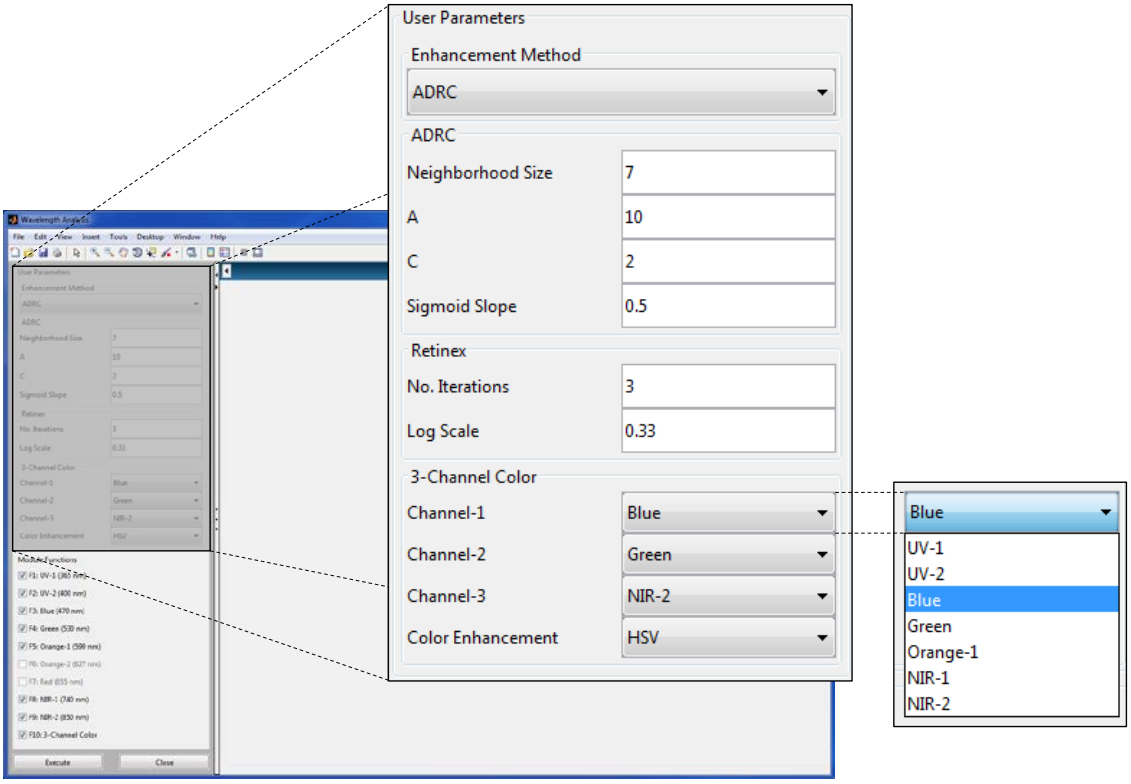

Figure 20. Close-up of a user parameters region

This region allows the user to change/set various algorithm parameters through the use of edit boxes and pull-down menus.

Module Functions

The *Module Functions* region of a data analysis panel is where the user selects and executes algorithms. User inputs in this region are provided by means of check boxes similar to those shown in Figure 21. In this region, the user simply selects functions he/she desires to apply to the current data set by checking the corresponding boxes. If a function requires the presence of a particular wavelength channel that is missing from the current data set, it is automatically disabled. An example of this is illustrated in Figure 21 where we see that functions *F6: Orange-2* and *F7: Red* have been disabled so they cannot be inadvertently selected. This logic was built-in to our GUI design to help guide the user in his/her selection of applicable functions.

Once the user is satisfied with his/her choice of parameter settings and functions, the *Execute* button is pressed to apply the list of functions to the current data set. After activation, *Execute* changes to *Running* indicating that functions are executing. Upon completion of the last function, *Running* changes back to *Execute* notifying the user that output images are ready to be reviewed. Note that all functions selected at the time the *Execute* button is pressed will be implemented. To close the panel, the user simply presses the *Close* push-button.

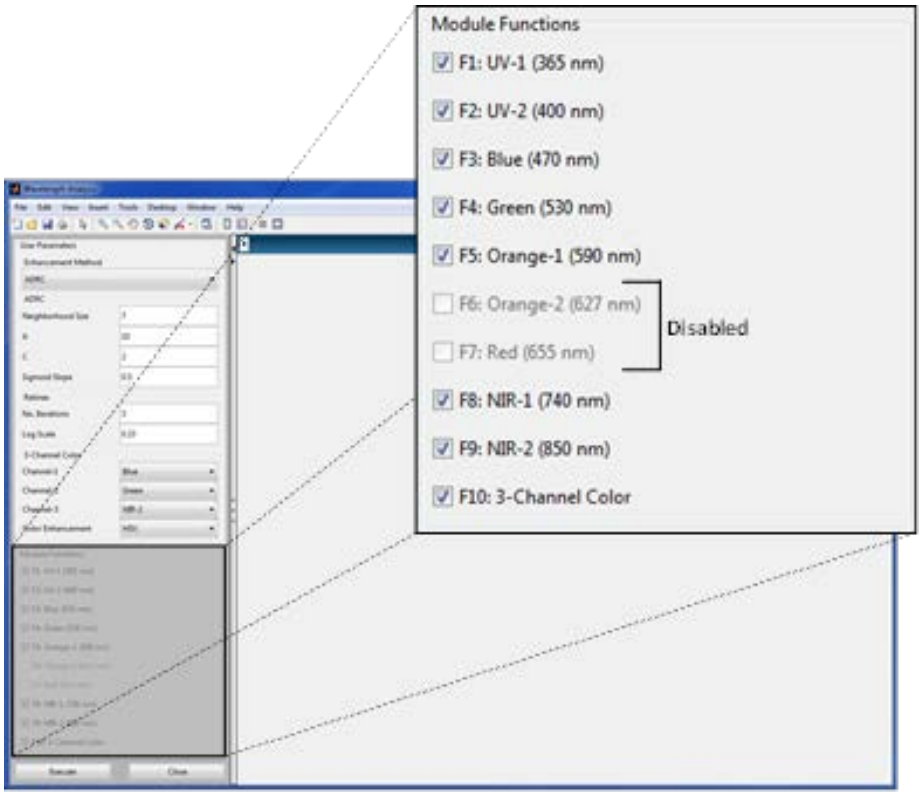

Figure 21. Close-up of a module function region

This region allows the user to select and execute specific data analysis algorithms

Image Display

The *Image Display* region of a data analysis panel is where algorithm results are displayed to the user. An example of this region is shown in Figure 22. A tabbed window is generated for each algorithm and labeled with the corresponding function number. Tabs appear in either the blue bar at the top of the panel or green bar at the bottom and control which window is visible. Tabs appearing in the green bar indicate that a module function generated multiple output images. The user can scroll through the available tabs using the left and right arrows located at the ends of the bars. Windows can be undocked from the image display region and opened in a new figure using the up-arrow located on the tabs. Undocked windows are returned to the image display region using the docking button located in the upper right region of the window. The standard MATLAB toolbar applications such as zoom in/out, pan, magnify, data cursor, etc. are also available for use to perform detailed examinations of the displayed image.

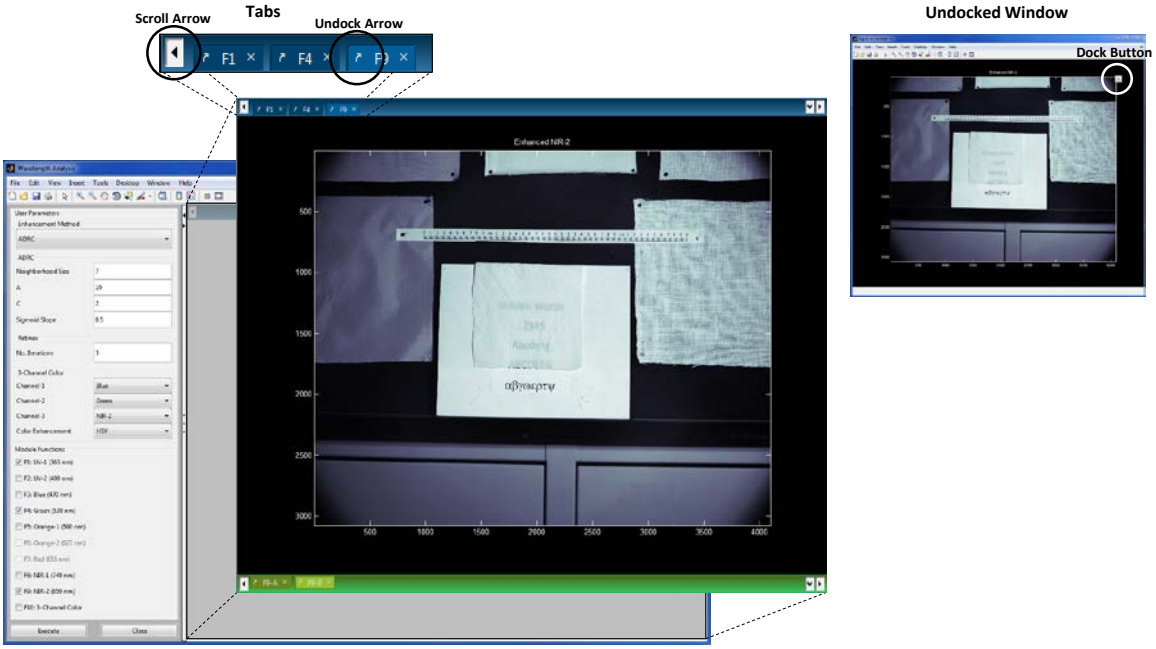

Figure 22. Close-up of an image display region

This region is where algorithm results are displayed to the user.

Main Image Analysis Panel

The main image analysis panel shown in Figure 23 allows the user to manipulate and examine data sets collected by the crime scene survey camera. It provides the user with several basic data manipulation functions: initialize system with default parameters, load image data set, select region-of-interest to process, correct lighting, and remove noise in UV channels. In addition, it gives the user access to five different data analysis methods to examine the current data set for traces of various chemicals and components. These analysis methods include: wavelength, false color, opponent color, spectral, texture, and quality metric. Every analysis method launches its own GUI panel to permit the user to change/set algorithm parameters and select functions. Each panel is discussed individually in the following sections.

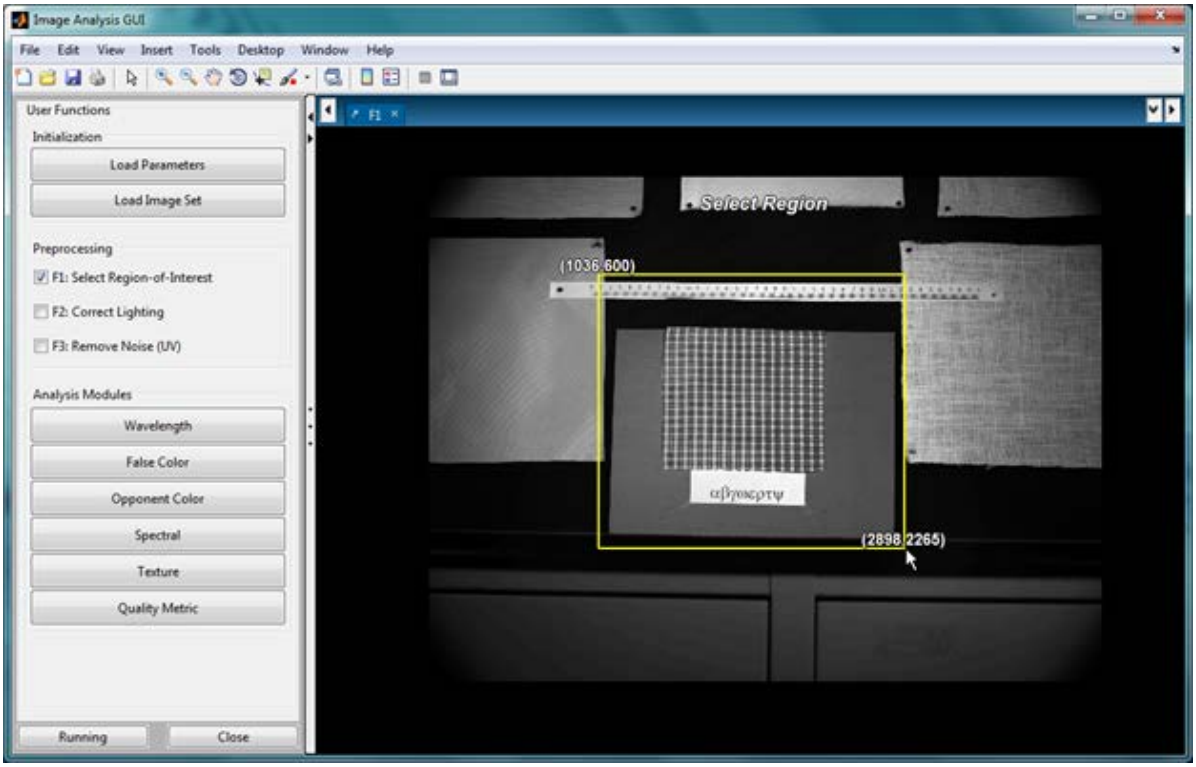

Figure 23. Example of the main algorithm analysis GUI panel

Wavelength Analysis

The *Wavelength Analysis Panel* provides the user access to two basic types of algorithms: contrast enhancement and pseudo color (see Figure 24). This panel allows the user to choose one of two contrast enhancement methods: adaptive dynamic range compression (ADRC) or retinex lighting model (Retinex). Selection is made through the *Enhancement Method* pull-down menu. Each algorithm has its own individual set of parameters that the user can manipulate and appear under their respective headings *ADRC* and *Retinex*. The selected enhancement method will be applied to checked functions listed in the *Module Function* region once the *Execute* button is pressed. Each function produces two tabbed windows: one displays an unprocessed image and the other a contrast enhanced version. For a detailed explanation of the contrast enhancement algorithms, the user is referred to Grant No. 2010-DN-BX-K144 final report, "Day and Night Real Time Signature Enhancement Crime Scene Survey Camera".

To generate a 3-channel, pseudo color image, the user chooses a wavelength from the *Channel-1*, *Channel-2*, and *Channel-3* pull-down menus. In addition, the user selects one of five color space models from the *Color Enhancement* menu. This parameter determines which color space transformation is used to convert the pseudo RGB image to a more biologically plausible color map for enhancement purposes. When the *F10: 3-Channel Color* function is checked, these settings are used to generate a pseudo color image. After the *Execute* button is pressed, two tabbed windows are produced: one displays an unprocessed color image and the other a contrast enhanced version.

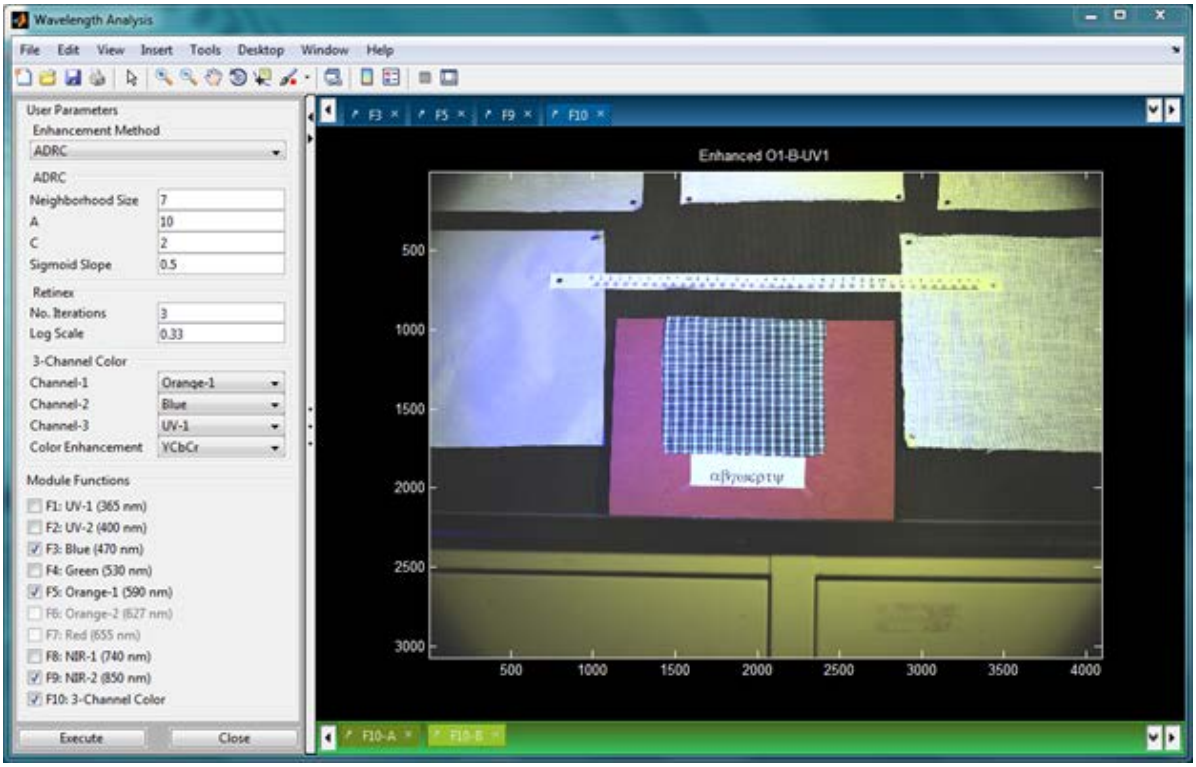

Figure 24. GUI panel for the wavelength analysis module

This panel uses pull-down menus to allow the user to select one of two enhancement methods: ADRC and Retinex. Algorithm parameters are changed/set by means of text edit boxes and pull-down menus which are initialized with default values. Basic wavelength images to be process are selected via check boxes. Enhancements are applied via the Execute button. Output results are presented in the image display region.

False Color Analysis

The *False Color Analysis Panel* provides eleven pseudo color processing techniques. These techniques differ from the *3-Channel Color* function in that color is generated from channel ratios and differences as opposed to just simple channel combinations. For a detailed explanation of the various false color algorithms, the user is referred to Grant No. 2010-DN-BX-K144 final report, "Day and Night Real Time Signature Enhancement Crime Scene Survey Camera". An example of a false color analysis panel is shown in Figure 25. Some of the images used for illustration are digitally zoomed in on the 'regions of interest' and may appear to have low resolution. In these cases, the entire high resolution images are not shown to avoid confusion.

Like the *Wavelength Analysis Panel*, this panel allows the user to choose one of two contrast enhancement methods: ADRC or Retinex. Selection is made through the *Enhancement Method* pull-down menu. Each algorithm has its own individual set of parameters that the user can manipulate and appear under their respective headings *ADRC* and *Retinex*. In addition, the user selects one of five color models from the *Color Enhancement* menu. This parameter

determines which color transformation is used to convert the pseudo RGB image to a more biologically plausible color map for enhancement purposes. The selected enhancement method will be applied to all checked functions in the *Module Function* region once the *Execute* button is pressed.

Depending on the wavelength combinations used by the functions, one to four tabbed windows will be produced. For functions requiring a UV channel, two images will be displayed: one for UV-1 and the other for UV-2. The same holds true for functions utilizing an NIR channel. One image will be generated using NIR-1 and another for NIR-2. If a function uses both UV and NIR channels, then four images will be generated, one for each combination of the two channels.

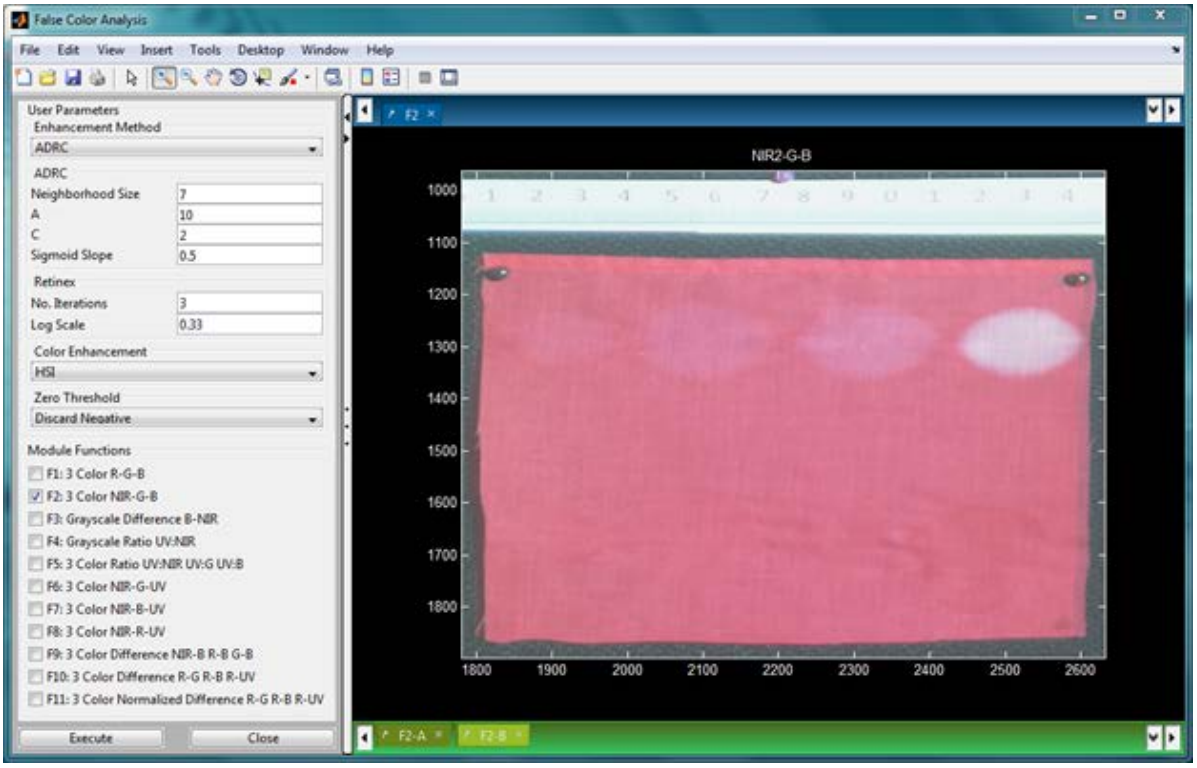

Figure 25. GUI panel for the false color analysis module

This panel uses pull-down menus to allow the user to select one of two enhancement methods: ADRC and Retinex. Algorithm parameters are input by means of text edit boxes and pull-down menus which are initialized with default values. False color processing methods are selected via check boxes. Selected algorithms are initiated via the Execute button. Output results are presented in the image display region.

Opponent Color Analysis

The *Opponent Color Analysis Panel* provides eight different color processing techniques for manipulating antagonistic color pairs (red-green, yellow-blue) to improve color perception and contrast. These techniques are grouped into four general classes: concentric single-opponent,

spatially opponent, broad-band, and double-opponent. For a detailed explanation of the various opponent color algorithms, the user is referred to Grant No. 2010-DN-BX-K144 final report, "Day and Night Real Time Signature Enhancement Crime Scene Survey Camera". An example of an opponent color analysis panel is shown in Figure 26.

This panel allows the user to choose three spectral images that are combined to form a pseudo RGB color image. The spectral images are selected using the *Channel-1*, *Channel-2*, and *Channel-3* pull-down menus listed under *Band Combinations*. In addition, the user must select one of five color models from the *Color Space* menu that will be used to improve signal-to-noise ratio and transform the RGB image to a more biologically acceptable color map for enhancement purposes. Since the underlying computational model for our opponent color processing is a feed-forward center-surround *Shunt Filter*, text edit boxes are provided so the user can change/set various filter parameters. Opponent color techniques are provided for each class and antagonistic color pair combination and are selected by means of check boxes in the *Module Function* region. All checked functions will be implemented once the *Execute* button is pressed.

Depending on the selected function either four or eight tabbed windows will be produced. Spatially-opponent and broad-band functions will generate four output images while single-opponent and double opponent methods will generate eight.

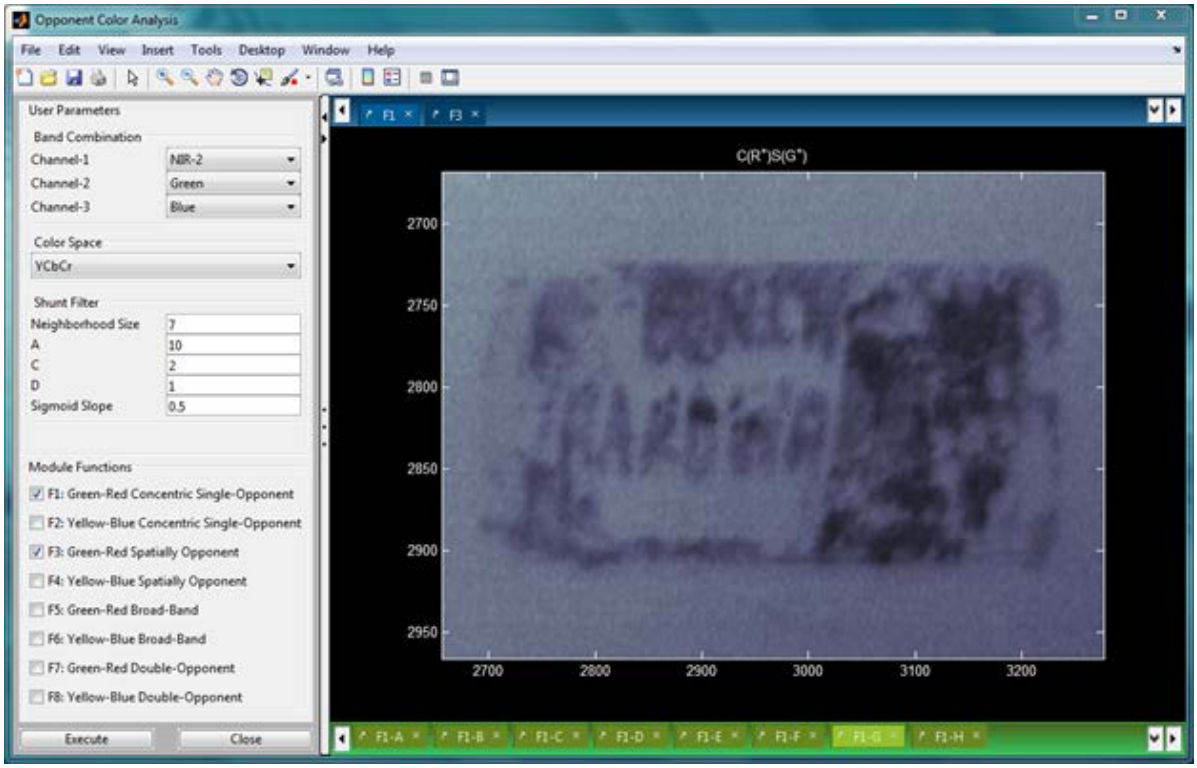

Figure 26. GUI panel for the opponent color analysis module

Algorithm parameters are changed/set by means of pull-down menus and text edit boxes which are initialized with default values. Opponent color processing methods are selected via check boxes. Selected algorithms are initiated via the Execute button. Output results are presented in the image display region.

Spectral Analysis

The *Spectral Analysis Panel* provides twenty data analysis techniques that combine and manipulate different spectral bands to enhance images and provide additional information not easily seen with a single wavelength. For a detailed explanation of the various spectral analysis algorithms, the user is referred to Grant No. 2010-DN-BX-K144 final report, "Day and Night Real Time Signature Enhancement Crime Scene Survey Camera". An example of a spectral analysis panel is shown in Figure 27.

This pane provides the user with two different groups of parameters: zero threshold and enhancement. Zero threshold determines the polarity of an image, i.e., generates a positive or negative image by either discarding negative or positive values within the image. It is used by specific functions and changed/set through their respective pull-down menus. Enhancement parameters remove noise spikes and improve image contrast and are applied across the board to all spectral functions. These values are input by means of text edit boxes. Spectral analysis algorithms are selected with check boxes in the *Module Function* region. All checked functions will be implemented once the *Execute* button is pressed.

Depending on the selected function either one or two tabbed windows will be produced. For functions requiring a UV channel, two images will be displayed: one for UV-1 and the other for UV-2. Similarly for functions utilizing an NIR channel, one image will be generated using NIR-1 and another for NIR-2.

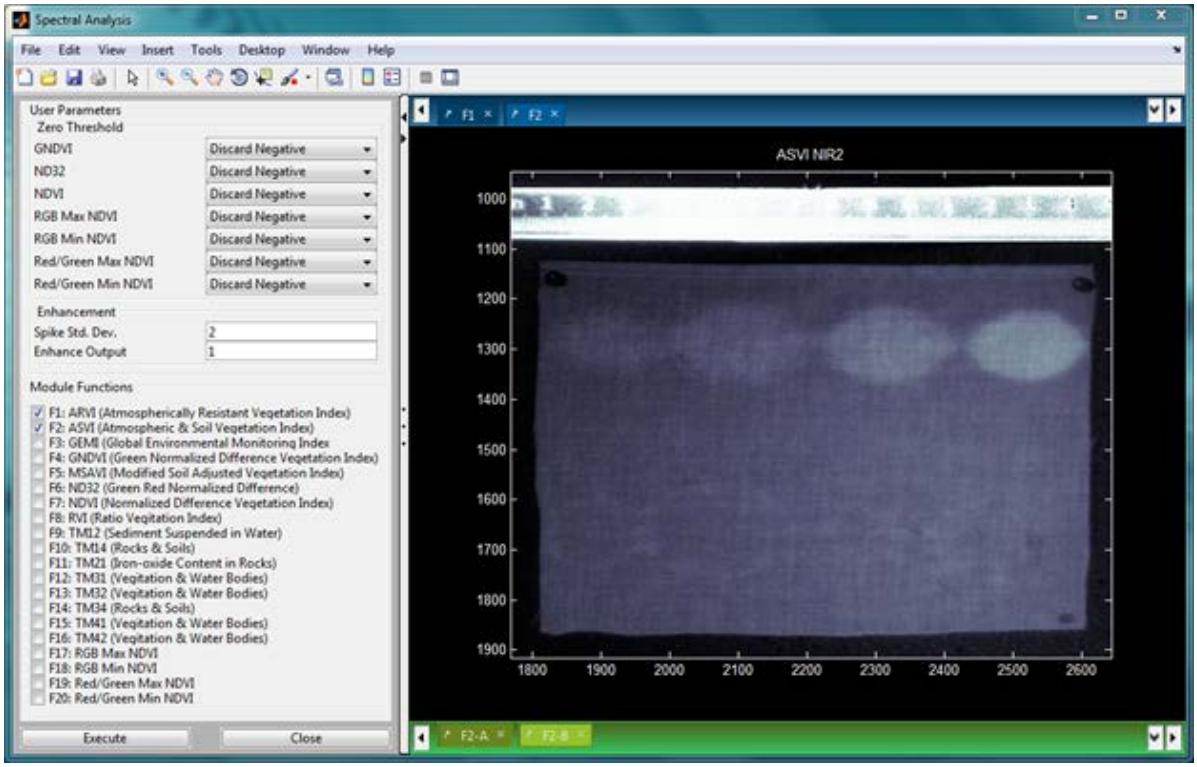

Figure 27. GUI panel for the spectral analysis module

Algorithm parameters are input by means of pull-down menus and text edit boxes which are initialized with default values. Spectral processing methods are selected via check boxes. Selected algorithms are initiated via the Execute button. Output results are presented in the image display region.

Texture Analysis

The *Texture Analysis Panel* provides four different texture enhancement techniques: composite wavelengths, orientation pyramid, steerable filters, and steerable pyramid. For a detailed explanation of the various texture analysis algorithms, the user is referred to Grant No. 2010-DN-BX-K144 final report, "Day and Night Real Time Signature Enhancement Crime Scene Survey Camera". An example of a texture analysis panel is shown in Figure 28.

Each texture enhancement technique has its own specific set of parameters which are listed in the *User Parameters* region under their respective heading: *Orientation Pyramid*, *Steerable Filters*, and *Steerable Pyramid*. These parameters are changed/set by means of text edit boxes and pull-down menus. The *Image Enhancement* parameter applies across the board to all texture analysis functions. It defines the sigmoid slope used in the preprocessing stage to contrast enhance all wavelength images prior to computation of the texture image. Texture analysis algorithms are selected with check boxes in the *Module Function* region. All checked functions will be implemented once the *Execute* button is pressed. A single tabbed window is generated for each texture function where its respective output image is displayed.

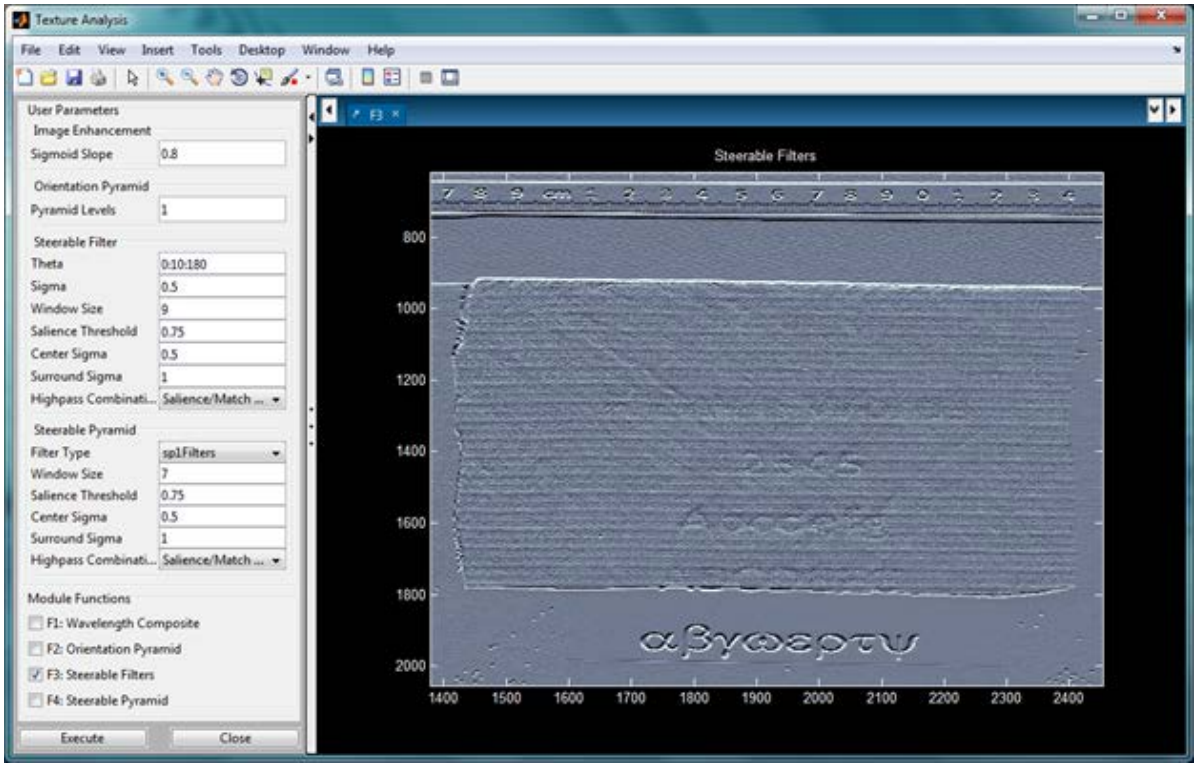

Figure 28. GUI panel for the texture analysis module

Algorithm parameters are changed/set by means of text edit boxes and pull-down menus which are initialized with default values. Texture processing methods are selected via check boxes. Selected algorithms are initiated via the Execute button. Output results are presented in the image display region.

Quality Metric Analysis

The *Quality Metric Analysis Panel* provides five image quality metrics: edge, corner, symmetry and contrast (ECSC); image contrast; edge, corner and symmetry (ECS); anisotropic quality index (AQI); and anisotropic quality index ponderated (AQIP). For a detailed explanation of the various metrics, the user is referred to Grant No. 2010-DN-BX-K144 final report, "Day and Night Real Time Signature Enhancement Crime Scene Survey Camera". An example of a quality metric analysis panel is shown in Figure 29.

Each quality metric has its own specific set of parameters which are listed in the *User Parameters* region under their respective heading: *Image Contrast Measure*, *ECSI/ECSCI*, and *AQI/AQIP*. These parameters are changed/set by means of text edit boxes. Note that ECSI and ECSCI share the same set of parameters as does AQI and AQIP. Image quality metrics are selected with check boxes in the *Module Function* region. All checked functions will be implemented once the *Execute* button is pressed. A single tabbed window is generated for each quality metric with the exception of image contrast measure, which generates two – one for histogram flatness and the other for histogram spread. For each metric, analyzed images are displayed in rank order from most significant content to least. Measured values are displayed above each image.

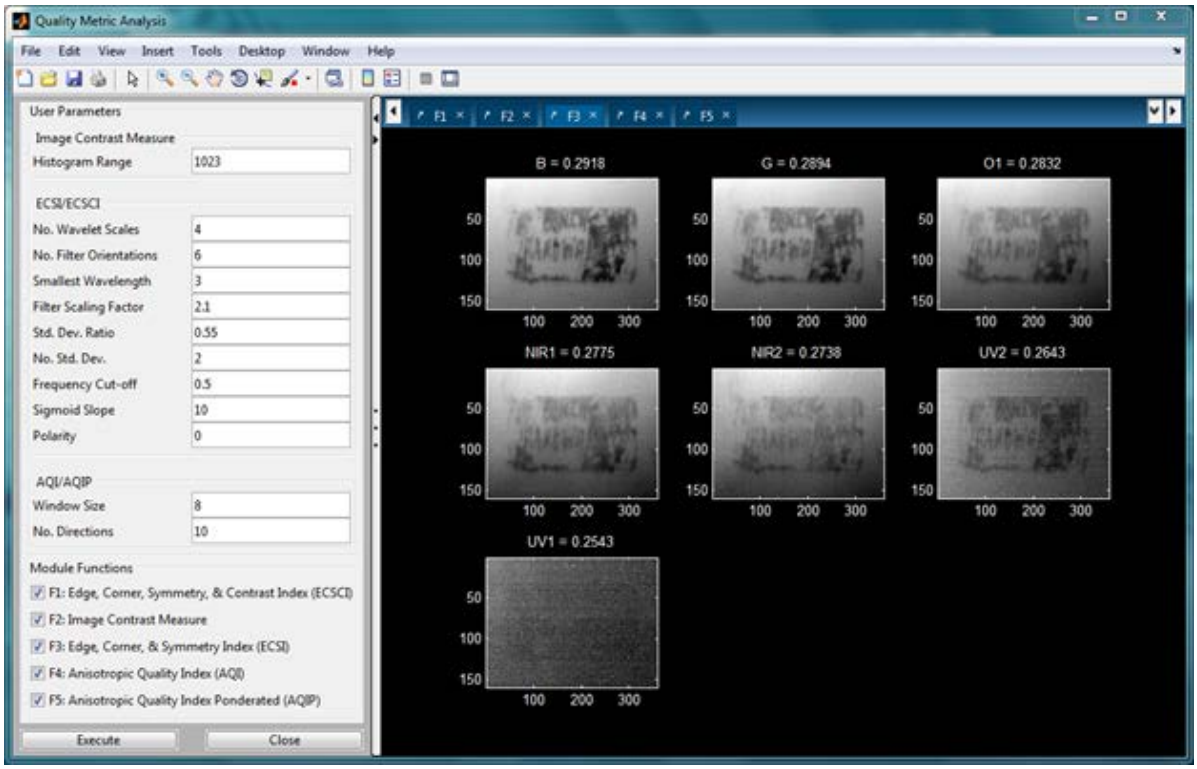

Figure 29. GUI panel for the quality metric analysis module

User defined parameters are provided by means of text edit boxes which are initialized with default values. Quality metric measures to be executed are selected via check boxes. Selected algorithms are initiated via the Execute button. Output results are presented in the image display region.

II.4.Experimental Procedure

We set up a test area in our laboratory. The camera and illuminators were mounted to standard photographic tripods. The relative geometry between sources, target and the screen could be varied easily with tripod mounting. The electronics box and a PC computer resided on an optics bench located nearby. The illuminators were tethered to the electronics box with three-meter-long cords that allowed freedom of locating them wherever desired. The camera (with the LCTF mounted to it) was located closer to the electronics box.

We set up test targets on a poster board and acquired sets of images as desired. The image acquisition GUI allowed complete control over the number of images, and the illumination/filter wavelengths. Recipes used included fluorescence as well as multispectral modes.

The UV LEDs were selected to be long wavelength (UV-A similar to black light) to be benign to DNA in the evidence, but they could still cause photochemical cataract and skin erythema (sunburn). Operators used polycarbonate UV eye protection and avoided direct contact with UV light. The visible strobes were also very bright (similar to photographer's flash) and direct exposure by looking into the illuminators was avoided.

We post processed the collected imagery to investigate if we could reveal information that was not easily captured by a color camera (Panasonic DMC-FZ20) or by the naked eye.

III. Results

III.1. First Multi-Spectral Data Collection

The target was a paper with some writing on it obscured by a piece of cloth pinned to a poster board. In addition to testing active multispectral imaging, we also hoped to exploit a known phenomenology relating to the ability of long wavelengths of light to penetrate through thin layers of material and image targets hidden below. This has very practical applications such as revealing targets painted over in order to destroy evidence, forgery cases, etc.

As we anticipated, the visible camera or naked eye could not decipher the writing or even realize that there was more writing behind the cloth. The two near infrared wavelengths however were able to reveal writing, and the longest wavelength allowed us to clearly read it.

While experimenting with the algorithms GUI, the residue from an obscure peeled-off label grabbed our attention. In this case the shorter wavelength images had more information than the longer wavelengths. In fact there was very little trace of the label residue at NIR wavelength (Figure 30 C). We were able to highlight the label residue with false colored images using two short wavelengths (blue and green) and near IR to be able to read the text. The peeled-off label had left behind sufficient residue to allow us to read the text that used to be on the label. See Figure 30.

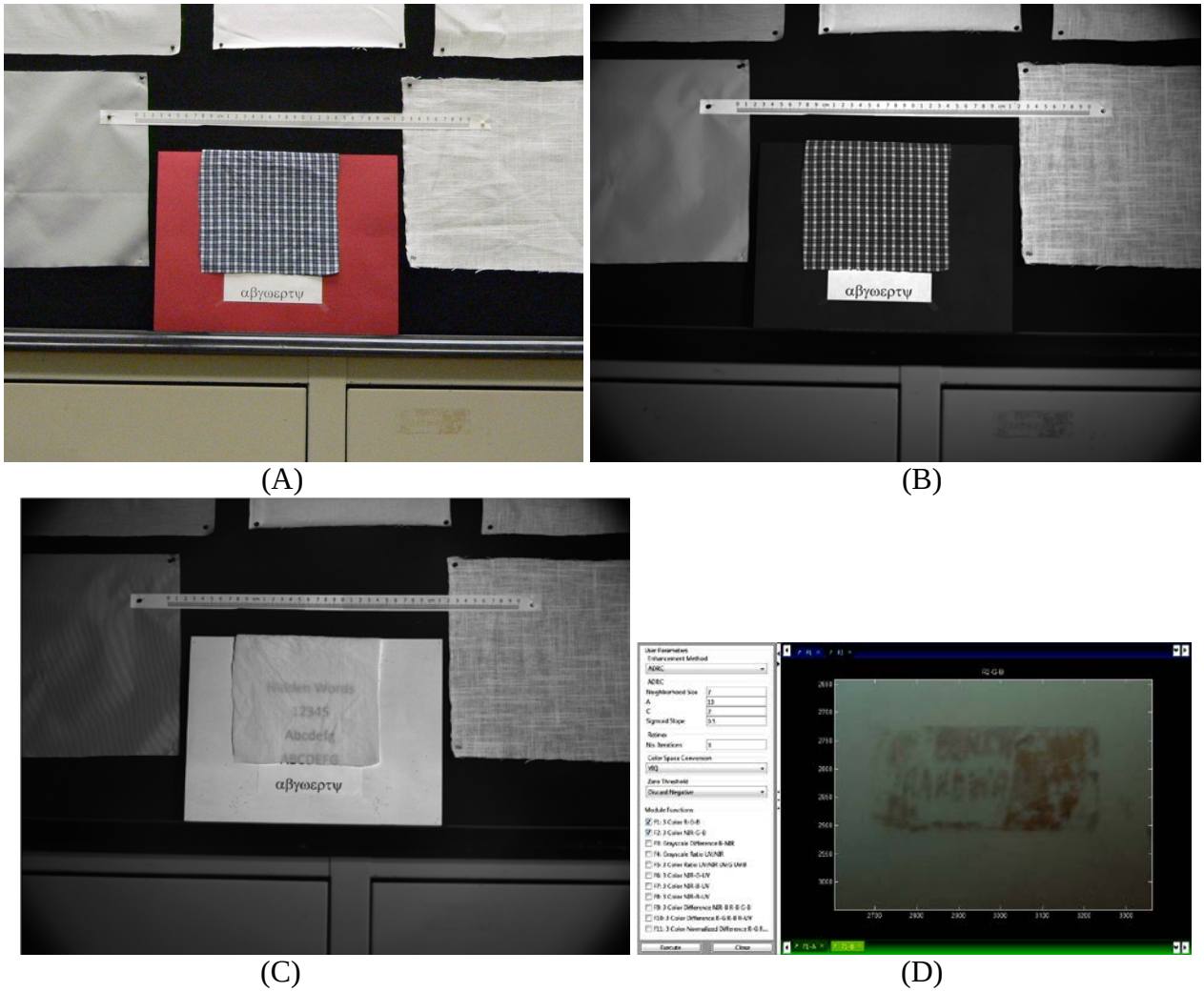

(A) (B)

(C) (D)

Figure 30. First multispectral images obtained with the brassboard system.

The target is a paper with some writing on it obscured by a piece of cloth. (A) is a color camera image, (B) is image in blue(470 nm). The writing is completely invisible to visible camera and at short wavelengths. Longer wavelengths penetrate the cloth and enable deciphering the text. (C) is infrared image (850 nm) where the text is most easily readable. During the experiment we noticed that there was a peeled-off sticker with a handwritten label on the right drawer, which was better visible at low wavelengths. False coloring algorithm using blue, green and NIR wavelengths enhanced the label to the extent, where the text B_NCH HARDWA (Likely BENCH HARDWARE) could be easily read (D).

III.2. Imaging Bleach and Bovine Blood Spots

We created an imaging test sample using blood and bleach on a red cloth background. The sample was created primarily to test the functionality of the fluorescence mode. Bleach is known to fluoresce and is often a false positive encountered in forensic applications. The sample has two rows of stains in increasing concentration of staining material from left to right. The dilution used DI water. The rightmost bleach spot is clearly visible to naked eye. The other three bleach spots and the strongest concentration blood spot (bottom right) can be picked out upon careful examination. The remaining three (bottom row left three) are not visible at all. It should be noted that the crimps in the cloth provide some hint of tampering even though spots are not visible. The

unprocessed color camera image fares slightly worse. It can pick up three bleach spots and the strongest blood spot.

We imaged the spot in the fluorescence mode where we used 365 nm as the illumination wavelength and scanned the LCTF across all wavelengths. The exposure times were allowed to be up to as long as 500 ms so the weak UV and fluorescent light at longer wavelengths could be collected. The best unprocessed image was the UV image where both the illumination and the LCTF states were at 365 nm. The bleach spots are much clearer than the visible camera image or naked eye perception. Only one very obscure blood spot is visible. The spectral algorithms (RVI and TM31- see [1] for algorithm references) derived from remote sensing applications worked quite well. Interestingly, these enhancements use red and NIR received wavelengths, as opposed to the UV image that worked best for bleach but not for blood. See Figure 31

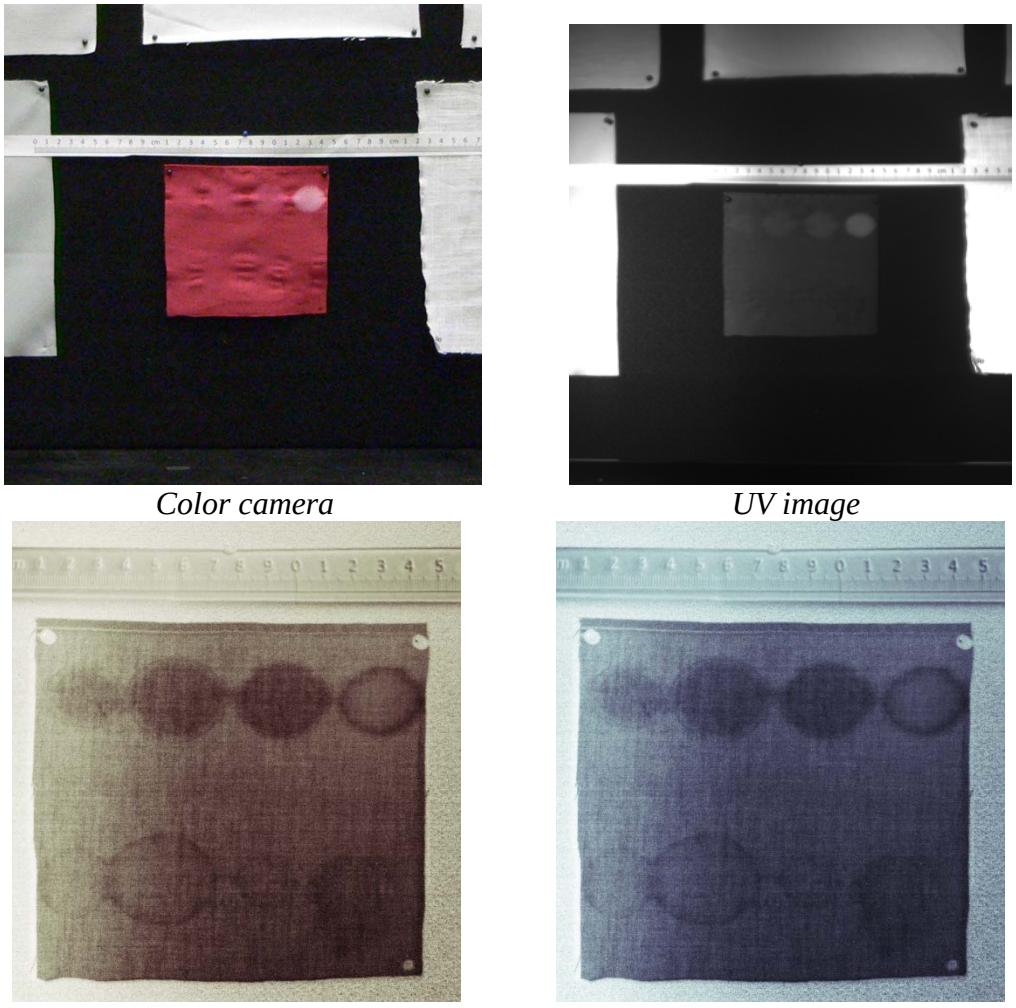

Color camera *UV image*

Spectral enhancement RVI *Spectral enhancement TM34*

Figure 31. UV/Fluorescent imaging of bleach and blood spots

UV Image (both illuminator and LCTF at 365 nm) shows a lot more detail of bleach but was not as successful in enhancing the blood spots. The spectral enhancement algorithms that use LCTF channels at red and NIR wavelengths successfully revealed and enhanced all eight spots.

IV. Conclusions

The primary goal of this project has been met. We have developed brassboard level hardware with performance upgrades to the camera, illumination, and tunable filter. The hardware is well packaged and is quite portable. We have developed two sufficiently user friendly software GUIs for image acquisition and image analysis, that will enable (with some training) operation by a researcher outside the TSI development team.

In the process, we have also demonstrated a novel liquid crystal tunable filter that is substantially better than off-the-shelf products in terms of UV/blue transmission, free spectral range and switching speed. High performance multispectral filters have applications beyond the forensic survey camera. Given we use processes and materials similar to those in use by consumer products; we believe there is insignificant cost consequence to achieving these performance benefits.

Proof of concept of phenomenology was established in the earlier project through a trade study involving numerous imaging experiments. A secondary goal has been to expand this trade study with additional imaging experiments with the new hardware. While we are testing the new hardware with imaging experiments, and plan to continue until we are out of project resources, we are limited by the available resources. Hardware and software development consumed more resources than we anticipated and we will look for additional (internal or external) resources to gain more experience with hardware and explore further improvements.

The versatility and programmability of the hardware means possible improvements can be numerous. The hardware is capable of collecting imagery significantly faster than it currently does through additional calibrations and software intelligence. In terms of image processing, the GUI relies on extensive user inputs. We would like to increase the level of automation in the future by using the quality metric analysis to select images with the highest information content and perform contrast enhancements through use of a knowledge base that selects algorithms most likely to produce the best results based on the target. The basic building blocks for all these upgrades are in place. Market analyses (for both integrated camera and LCTF) and technology transition through development of a prototype are critical steps for going beyond the current hardware/software version.

The impact on the practice and policy of criminal justice, both at local and national level, has tremendous potential to be an overreaching one. The technology, when fully developed, can answer the need for rapid crime scene scanning using multiple imaging modalities to identify targets of interest.

Furthermore, it enables the first investigators on the scene to operate in ambient lighting, and with minimal scene conditioning. The technology can provide, in a small, rugged, affordable, and portable device some of the extensive capabilities currently available only in the laboratory. This will result in improved onsite presumptive analysis of forensic evidence at the crime scene. The advanced minimally labor-intensive capability to detect forensic evidence at a crime scene at a distance can also overcome scene hazards and prevent evidence contamination.

V. Dissemination of Research Findings

The dissemination activity for this project has just begun. We have been providing informal updates in telephone discussions with our points of contact at Forensic Technology Center of Excellence at RTI international.

We have briefed the project to a Teledyne Scientific consultant whose assignment is to help sell our technology, services and products to commercial companies. We are particularly interested (due to his background) in soliciting help on identifying applications for the high performance LCTF. We plan to disseminate the findings in suitable conference meetings in the fields of optics/ optical engineering and forensic science. The dissemination activity will continue beyond the project period.

VI. References

1. M. Mahajan, et al., "Day and Night Real Time Signature Enhanced Crime Scene Survey Camera," Final report, Grant # 2010-DN-BX-K144, from National Institute of Justice
2. G. Reis, "Photoshop CS3 for Forensics Professionals," Sybex 2007
3. J. Schneider, "Forensic imaging goes digital," Forensic magazine, Dec 2006 /Jan 2007
4. A. Lin, "Forensic Applications of Infrared Imaging for the Detection and Recording of Latent Evidence," Journal of Forensic Sciences, Vol. 52, 5, pp1148 (2007)
5. Product literature for FAL3000 Alternate Light Source Kit: http://www.faurotforensics.com
6. D. McGraw, "New LEDs Enable Innovations in Forensic Alternative Light Sources," Forensic magazine, Jun/Jul 2005
7. C. J. Guffey, "Laser Technology: Revolutionizing CSI Work," Forensic magazine, Oct/Nov 2007
8. Product literature for SceneScope Advanced RUVIS UV Imager: www.crimescope.com
9. S. Milutin, "Detection of Semen and Blood Stains Using Polilight as a Light Source," Forensic Science International, Vol. 51, p. 289 (1991)
10. N. Vandenberg, et al, "The Use of Polilight in the Detection of Seminal Fluid, Saliva, and Bloodstains and Comparison with Conventional Chemical-Based Screening Tests," Journal of Forensic Science JFSCA. Vol. 51, 2, pp 361 (2006)
11. Product literature for Crime-Lite 80L: www.fosterfreeman.com
12. S. Lin, et al, "Polarization- and Specular-Reflection-Based, Non-contact Latent Fingerprint Imaging and Lifting," Journal of the Optical Society of America A, Vol. 23, 9, pp. 2137 (2006)
13. Leica HDS Laser Scanners product literature
14. Panoscan product literature
15. T. Amano, et al., "Fluorescence Spectra from Human Semen and Their Relationship with Sperm Parameters," Systems Biology in Reproductive Medicine.1996, Vol. 36, No. 1 : Pages 9-15

16. Bramble S.K., et al., “Ultraviolet luminescence from latent fingerprints (1993),” Forensic Science International, 59 (1), pp. 3-14

17. A. Fiedler, et al., “Detection of Semen (Human and Boar) and Saliva on Fabrics by a Very High Powered UV-/VIS-Light Source,” The Open Forensic Science Journal (2008) 1:12-15

18. H.J. Kobus, et al., “Improving the Effectiveness of Fluorescence for the Detection of Semen Stains on Fabrics,” Journal of Forensic Science, Vol. 47, p.823 (2002)

19. Leiner M.J.P., et al., “The total fluorescence of human urine,” Analytica Chimica Acta, 198 (C), pp. 13-23 (1987)

20. S. Lowndes, “Blood Interference in Fluorescence Spectrum: Experiment, analysis and comparison with intraoperative measurements on brain tumor,” Bachelor Thesis. Institute for Medical and Analytical Technologies (IMA), FHNW, Switzerland. Department of Biomedical Engineering (IMT), Linköping University, Sweden. Linköping, April - June 2010

21. L.S. Powers, et al., “Method and apparatus for detecting and imaging the presence of biological materials,” US Pat 7,186,990 B2, 2004

22. Nikolaos S Soukos, et al., “A rapid method to detect dried saliva stains swabbed from human skin using fluorescence spectroscopy,” Forensic Science International. Volume 114, Issue 3, Pages 133-138, 11 December 2000

23. Springer E., et al., “Detection of dry body fluids by inherent short wavelength UV luminescence: Preliminary results,” Forensic Science International, 66 (2), pp. 89-94(1994)

24. G. C. Tang, et al., “Laser fluorescence spectroscopy from human spermatozoa,” Applied Optics , Vol. 32, No. 4 / 1 February 1993

25. Virkler K et al., “Analysis of body fluids for forensic purposes: From laboratory testing to non-destructive rapid confirmatory identification at a crime scene,” Forensic Science International 2009 March; 188:1-17

26. John H. Wagner et al., “Background Correction in Forensic Photography I. Photography of Blood under Conditions of Non-Uniform Illumination or Variable Substrate Color—Theoretical Aspects and Proof of Concept,” J Forensic Sci, Vol. 48, No. 3, May 2003

27. Markus Duelli et al., “Polarization recovery system based on light pipes,” Proc. SPIE 4657, Projection Displays VIII, 9 (April 30, 2002)

28. Thorlabs: KURIOS-WB1 Liquid crystal tunable filter product literature

29. Perkin Elmer VariSpec LC Tunable Filters product literature

30. Yu-Hua Lin, et al., "Compact 4 cm aperture transmissive liquid crystal optical phased array for free-space optical communications", Proceedings of SPIE Vol. 5892, SPIE, Bellingham, WA, 2005

31. Milind Mahajan et al., “Voltage calibration of dual-frequency liquid crystal devices for infrared beam steering applications", Proceedings of SPIE Vol. 5892, SPIE, Bellingham, WA, 2005

32. Pochi Yeh, Optical Waves in Crystals, Wiley Interscience, p.121

33. Hecht E., Optics, Addison Wesley, fourth edition, chapter 8